Distribution of planktonic biogenic carbonate organisms in the Southern Ocean south of Australia: a baseline for ocean acidification impact assessment

Thomas W. Trull[1,2,3], Abraham Passmore[1,2], Diana M. Davies[1,2], Tim Smit[4], Kate Berry[1,2], and Bronte Tilbrook[1,2]

1. Climate Science Centre, Oceans and Atmosphere, Commonwealth Scientific and Industrial Research Organisation, Hobart, 7001, Australia
2. Antarctic Climate and Ecosystems Cooperative Research Centre, Hobart, 7001, Australia
3. Institute of Marine and Antarctic Studies, University of Tasmania, Hobart, 7001, Australia
4. Utrecht University, Utrecht, 3508, Holland

Correspondence to: Tom Trull (Tom.Trull@csiro.au)

Abstract

The Southern Ocean provides a vital service by absorbing about one sixth of humankind's annual emissions of CO_2. This comes with a cost – an increase in ocean acidity that is expected to have negative impacts on ocean ecosystems. The reduced ability of phytoplankton and zooplankton to precipitate carbonate shells is a clearly identified risk. The impact depends on the significance of these organisms in Southern Ocean ecosystems, but there is very little information on their abundance or distribution. To quantify their presence, we used coulometric measurement of particulate inorganic carbonate (PIC) on particles filtered from surface seawater into two size fractions: 50-1000 μm to capture foraminifera (the most important biogenic carbonate forming zooplankton) and 1-50 μm to capture coccolithophores (the most important biogenic carbonate forming phytoplankton). Ancillary measurements of biogenic silica (BSi) and particulate organic carbon (POC) provided context, as estimates of the biomass of diatoms (the highest biomass phytoplankton in polar waters), and total microbial biomass, respectively. Results for 9 transects from Australia to Antarctica in 2008-2015 showed low levels of PIC compared to northern hemisphere polar waters. Coccolithophores slightly exceeded the biomass of diatoms in Subantarctic waters, but their abundance decreased more than 30-fold poleward, while diatom abundances increased, so that on a molar basis PIC was only 1% of BSi in Antarctic waters. This limited importance of coccolithophores in the Southern Ocean is further emphasized in terms of their associated POC, representing less than 1 % of total POC in Antarctic waters and less than 10% in Subantarctic waters. NASA satellite ocean colour based PIC estimates were in reasonable agreement with the shipboard results in Subantarctic waters, but greatly over-estimated PIC in Antarctic waters. Contrastingly, the NASA Ocean Biogeochemical Model (NOBM) shows coccolithophores as overly restricted to Subtropical and northern Subantarctic waters. The

cause of the strong southward decrease in PIC abundance in the Southern Ocean is not yet clear. Poleward decrease in pH is small and while calcite saturation decreases strongly southward it remains well above saturation (>2). Nitrate and phosphate variations would predict a poleward increase. Temperature and competition with diatoms for limiting iron appear likely to be important. While the future trajectory of coccolithophore distributions remains uncertain, their current low abundances suggest small impacts on overall Southern Ocean pelagic ecology.

1. Introduction

Production of carbonate minerals by planktonic organisms is an important and complex part of the global carbon cycle and climate system. On the one hand, carbonate precipitation raises the partial pressure of CO_2 reducing the uptake of carbon dioxide from the atmosphere into the surface ocean; on the other hand, the high density and slow dissolution of these minerals promotes the sinking of associated organic carbon more deeply into the ocean interior increasing sequestration [*P.W. Boyd and Trull*, 2007b; *Buitenhuis et al.*, 2001; *Klaas and Archer*, 2002; *Ridgwell et al.*, 2009; *Salter et al.*, 2014]. Carbonate production is expected to be reduced by ocean acidification from the uptake of anthropogenic CO_2, with potentially large consequences for the global carbon cycle and ocean ecosystems [*Orr et al.*, 2005; *Pörtner et al.*, 2005].

The low temperature and moderate alkalinity of Southern Ocean waters make this region particularly susceptible to ocean acidification, to the extent that thresholds such as undersaturation of aragonite and calcite carbonate minerals will be crossed sooner than at lower latitudes [*Cao and Caldeira*, 2008; *McNeil and Matear*, 2008; *Shadwick et al.*, 2013]. Carbonate forming organisms in the Southern Ocean include coccolithophores (the dominant carbonate forming phytoplankton; e.g. [*Rost and Riebesell*, 2004]), foraminifera (the dominant carbonate forming zooplankton; e.g. [*Moy et al.*, 2009; *Schiebel*, 2002]), and pteropods (a larger carbonate forming zooplankton, which can be an important component of fish diets; e.g. [*Doubleday and Hopcroft*, 2015; *Roberts et al.*, 2014]). However, the importance of carbonate forming organisms relative to other taxa is unclear in the Southern Ocean [*Watson W. Gregg and Casey*, 2007b; *Holligan et al.*, 2010]. Satellite reflectance observations, mainly calibrated against northern hemisphere PIC results, suggest the presence of a "Great Calcite Belt" in Subantarctic waters in the Southern Ocean , and also show high apparent PIC values in Antarctic waters [*W M Balch et al.*, 2016; *W M Balch et al.*, 2011]. Our surveys were designed in part to evaluate these assertions for waters south of Australia.

As a simple step towards quantifying the importance of planktonic biogenic carbonate forming organisms in the Southern Ocean, we determined the concentrations of particulate inorganic carbonate (PIC) for two size classes, representing coccolithophores (1-50 μm, referred to as PIC01) and foraminifera (50-1000 μm, referred to as PIC50), from surface water samples collected on 9 transects between Australia and Antarctica. We provide ecological context for these observations based on the abundance of particulate organic carbon (POC) as a measure of total microbial biomass, and biogenic silica (BSi), the other major phytoplankton biogenic mineral, as a measure of diatom biomass. This provides a baseline assessment of the importance of calcifying plankton in the Southern Ocean south of Australia, against which future levels can be compared.

In the discussion of our results, we interpret BSi as representative of diatoms, PIC50 as representative of foraminifera, and PIC01 as representative of coccolithophores, including a tendency to equate this with the distribution of the most cosmopolitan and best studied coccolithophore, *Emiliania huxleyi*. These assumptions need considerable qualification. Most BSi is generated by diatoms (~90%), with only minor contributions from radiolaria and choanoflagellates in the upper ocean, making this approximation reasonably well supported [*Hood et al.*, 2006]. Similarly, but less certainly, foraminifera are a major biogenic carbonate source in the 50-1000 μm size range, but pteropods, ostrocods, and other organisms are also important [*Schiebel*, 2002]. We do not discuss the PIC50 results in any detail because of this complexity, because controls on foraminifera distributions appear to involve strongly differing biogeography of several co-dominant taxa, rather than dominance by a single species [*Be and Tolderlund*, 1971], because the numbers of these organisms collected by our procedures were small, and because assessing these issues is beyond the scope of this paper. Attributing all the PIC01 carbonate to coccolithophores relies on the assumption that fragments of larger organisms are not important. This seems reasonable given that the larger PIC50 fraction generally contained 10-fold lower PIC concentrations (as revealed in the Results section).

Our tendency to equate the PIC01 fraction with the abundance of *Emiliania huxleyi* is probably the weakest approximation. It is not actually central to our conclusions, except to the extent that we compare our PIC01 distributions to expectations based on models that use physiological results mainly derived from experiments with this species. That said, this is a poor approximation in Subtropical waters where the diversity of coccolithophores is large, but improves southward where the diversity decreases (see Smith et al. 2017 for recent discussion), and many observations have found that *Emiliania huxleyi* was strongly dominant in Subantarctic and Antarctic Southern Ocean populations, generally >80% [*Boeckel et al.*, 2006; *Eynaud et al.*, 1999; *Findlay and Giraudeau*, 2000; *Gravalosa et al.*, 2008; *Mohan et al.*, 2008]. Of course, *Emiliania huxleyi* itself comes in several strains even in the Southern Ocean, with differing physiology, including differing extents of calcification [*Cubillos et al.*, 2007; *M. N. Muller et al.*, 2015; *M.N. Muller et al.*, 2017; *Poulton et al.*, 2013; *Poulton et al.*, 2011]. All these approximations are important to keep in mind in any generalization of our results. We also note that our technique does not distinguish between living and non-living biomass, and thus is more representative of the history of production than the extent of extant populations at the time of sampling.

2. Methods

Sub-sections 2.1 and 2.2 present the sampling and analytical methods, respectively, used for the 8 transits across the Southern Ocean since 2012. Sub-section 2.3 details the different methods used during the earlier single transit in 2008 and assesses the comparability of those results to the later voyages. Sub-section 2.4 details measurements of water column dissolved nutrients, inorganic carbon

and alkalinity. Sub-section 2.5 provides details of satellite remote sensing data and the NASA Ocean Biogeochemical Model used for comparison to the ship results.

2.1. Voyages and sample collection procedures

The locations of the voyages, divided into north and south legs, are shown in Figure 1. Voyage and sample collection details are given in Table 1, where for ease of reference we have numbered the legs in chronological order and refer to them hereafter as VL1, VL2, etc. Samples were collected from the Australian icebreaker *RV Aurora Australia* for 4 voyages and from the French Antarctic resupply vessel *l'Astrolabe* for 1 voyage. All samples were collected from the ships' underway "clean" seawater supply lines with intakes at ~4 m depth. These supply lines are separate from the engine intakes, have scheduled maintenance and cleaning, and are only turned on offshore (to avoid possible contamination from coastal waters). Samples were collected primarily while underway, except during VL1 and VL3, which were operated as WOCE/CLIVAR hydrographic sections with full depth CTDs, with samples collected on station.

For all voyages (except VL1, discussed in section 2.3 below), separate water volumes were collected for the PIC, POC, and BSi analyses. The POC samples also yielded particulate nitrogen results - referred to here as PON. The POC/PON and BSi samples were collected using a semi-automated system that rapidly, ~ 1 minute, and precisely filled separate 1 L volumes for each analyte - thus these samples are effectively point samples. In contrast, PIC samples were collected using the pressure of the underway seawater supply to achieve filtration of large volumes (10's to 100's of litres) over ~2 hours. Thus these samples represent collections along ~20 miles of the ship track (except when done at stations).

POC/PON samples were filtered through pre-combusted 13 mm diameter quartz filters (0.8 µm pore size, Sartorius Cat#FT-3-1109-013) that had been pre-loaded in clean (flow-bench) conditions in the laboratory into in-line polycarbonate filter holders (Sartorius #16514E). The filters were preserved by drying in their filter holders at 60°C for 48 hours at sea, and returned to the laboratory in clean dry boxes.

Biogenic silica samples were filtered through either 13 mm diameter nitrocellulose filters (0.8 µm pore size, Millipore Cat#AAWP01300) or 13 mm diameter polycarbonate filters (0.8 µm pore size, Whatman Cat#110409), pre-loaded in clean (flow-bench) conditions in the laboratory into in-line polycarbonate filter holders (Sartorius #16514E). Filters were preserved by drying in their filter holders at 60°C for 48 hours at sea, and returned to the laboratory in clean dry boxes.

PIC samples were collected by sequential filtration for two size fractions. After pre-filtration through a 47 mm diameter 1000 μm nylon mesh and supply pressure reduction to 137 kPa, seawater was filtered through a 47 mm diameter in-line 50 μm nylon filter to collect foraminifera, and then through a 47 mm diameter in-line 0.8 μm GF/F filter (Whatman Cat#1825-047) to collect coccolithophores. The flow path was split using a pressure relief valve set to 55 kPa, so that large volumes (~200 L) passed the 50 μm filter, and only a small fraction of this volume (~15 L) passed the 0.8 μm filter. Filtration time was typically 2 hours. Volume measurement was done by either metering or accumulation. Based on visual examination, the high flow rate through the 50 μm nylon mesh was sufficient to disaggregate faecal pellets and detrital aggregates. The flow rate data also suggests that filter clogging was uncommon (see the Supplementary Information for expanded discussion). While still in their holders, the filters were rinsed twice with 3 mL of 20 mM potassium tetraborate buffer solution (for the first couple of voyages and later degassed deionized water) to remove dissolved inorganic carbon, and blown dry with clean pressurised air (69 kPa). We consider that the short contact time of this rinse did not dissolve PIC, based on the sharp (non-eroded) features of coccolithophores collected in this way and examined by scanning electron microscopy (Cubillos et al., 2007). The filters were then removed from their holders, folded, and inserted into Exetainer glass tubes (Labco Cat #938W) and dried at 60 °C for 48 hours for return to the laboratory. In the following text, we refer to the GF/F filter sample results (which sampled the 0.8 (~ 1) to 50 μm size fraction) as PIC01, and the nylon mesh sample fraction (which sampled the 50-1000 μm size fraction) as PIC50.

2.2 Sample analyses

2.2.1 Particulate Organic Carbon and Nitrogen analysis

The returned filter holders were opened in a laminar flow bench. Zooplankton were removed from the filters and the filters were then cleanly transferred into silver cups (Sercon Cat#SC0037), acidified with 50 μL of 2 N HCl and incubated at room temperature for 30 minutes to remove carbonates, and dried in an oven at 60 °C for 48 hours. The silver cups were then folded closed and the samples, along with process blanks (filters treated in the same way as samples, but without any water flow onboard the ship) and casein standards (Elemental Microanalysis OAS standard CatNo. B2155, Batch 114859) were sent to the University of Tasmania Central Sciences Laboratory for CHN elemental analysis against sulphanilamide standards. Repeat samples collected sequentially at approximately 2 hour intervals while the ship remained on station (station replicates) had a standard error of 7% (1 sd n= 10) and 8% (1 sd n= 10) for POC and PON respectively. Importantly the processing blanks were large and variable, and were corrected for separately for each voyage. For VL2 and VL3, POC process blanks averaged 25± 6 μg C (1 sd, n=2) equating to 20% of the average sample value. For VL4 and VL5, POC process blanks averaged 14 ± 2 μg C (1 sd, n=4) equating to 18% of the average sample

value. For VL6 and VL7, POC process blanks averaged 23 ± 3 µg C (1 sd n=4) equating to 28 % of the average sample value. For VL8 and VL9 POC process blanks averaged 14 ± 1 µg C (1 sd n=4) equating to 14 % of the average sample value.

2.2.2 Biogenic Silica analysis

Biogenic silica was dissolved by adding 4 mL of 0.2 M NaOH and incubating at 95 °C for 90 minutes, similar to the method of [*Paasche*, 1973]. Samples were then rapidly cooled to 4 °C and acidified with 1 mL of 1 M HCl. Thereafter samples were centrifuged at 1880 *g* for 10 minutes and the supernatant was transferred to a new tube and diluted with 36 g L^{-1} sodium chloride. Biogenic silica concentrations were determined by spectrophotometry using an Alpkem model 3590 segmented flow analyser and following USGS Method I-2700-85 with these modifications: ammonium molybdate solution contained 10 g L^{-1} $(NH_4)_6Mo_7O_{24}$, 800 µl of 10% sodium dodecyl sulphate detergent replaced Levor IV solution, acetone was omitted from the ascorbic acid solution, and sodium chloride at the concentration of seawater was used as the carrier solution. Station replicates had a standard error of 9% (1 sd n=9). The average blank values were 0.002 ± 0.003 µmoles per filter (1 sd, n=13) for nitrocellulose filters and 0.002 ± 0.002 µmoles per filter (1 sd, n=2) for polycarbonate filters, equating to 0.16 % and 0.01 % of average sample values, respectively.

2.2.3 Particulate Inorganic Carbon analysis

Particulate inorganic carbon samples were analysed by coulometry using a UIC CM5015 coulometer connected to a Gilson 232 autosampler and syringe dilutor. The samples were analysed directly in their gas tight Exetainer collection tubes, by purging for 5 minutes with nitrogen gas, acidification with 1.6 mL (PIC50 - 50 µm nylon filters) or 2.4 mL (PIC01 - GF/F filters) of 1 N phosphoric acid, and equilibration overnight at 40°C. Samples were analysed the following day with a sample analysis time of 8 minutes and a dried carrier gas flow rate of 160 mL min^{-1}. Calcium carbonate standards (Sigma Cat#398101-100G) were either weighed onto GF/F filters or weighed into tin cups (Sercon Cat# SC1190) and then inserted into Exetainer tubes (some with blank nylon filters). Station replicates had standard errors of 18% (1 sd n=11) and 13% (1 sd n=11) for PIC01 and PIC50 respectively. The average GF/F filter blank value was -0.07 ± 0.27 µg C (1 sd, n=47) equating to -- 0.21% of average sample values, and for nylon filters was 0.04 ± 0.27 µg C (1 sd, n=46) equating to 0.05% of average sample values.

2.3 Distinct sample collection and analytical methods used during V1

2.3.1 Distinct sample collection procedures for VL1

For VL1, single samples were collected at each location by both sequential filtration and centrifugation of the underway supply over 1-3 hours. Despite the long collection times these samples are effectively point samples because they were collected on station.

Sequential filtration was done using in-line 47 mm filter holders (Sartorius, Inc.) holding 3 sizes of nylon mesh (1000 µm, 200 µm, 50 µm) followed by a glass fibre filter (Whatman GF/F, 0.8 µm nominal pore size, muffled before use). These size fractions were intended to collect foraminifera (50-200 µm) and coccolithophores (0.8-50 µm), and pteropods (200-1000 µm), but the largest size fraction had insufficient material for analysis. The flow rate at the start of filtration was 25-30 L $hour^{-1}$ and typically dropped during filtration. The 0.8 µm filter was replaced if flow rates dropped below 10 L $hour^{-1}$. Sampling typically took 3 hours. Quantities of filtered seawater were measured using a flow meter (Magnaught M1RSP-2RL) with a precision of +/-1%. After filtration, remaining seawater in the system was removed using a vacuum pump. Filters were transferred to 75 mm Petri dishes inside a flow bench, placed in an oven (SEM Pty Ltd, vented convection) for 3-6 hours to dry at 60 ^{o}C and stored in dark, cool boxes for return to the laboratory.

A continuous flow Foerst type centrifuge [*Kimball Jr and Ferguson Wood*, 1964], operating at 18700 rpm, was used to concentrate phytoplankton from the underway system at a flow rate of 60 L per hour, measured using a water meter with a precision of +/-1% (Arad). Sampling typically took 1-3 hours. After centrifugation, 500 mL of de-ionized water was run through the centrifuge to flush away remaining seawater and associated dissolved inorganic carbon. This was followed by 50 mL of ethanol to flush away the de-ionized water, ensure organic matter detached from the cup wall, and speed subsequent drying. Inside a laminar flow clean bench, the slurry in the centrifuge head was transferred into a 10 mL polypropylene centrifuge tube (Labserve) and the material on the wall of the cup was transferred using 3 mL of ethanol and a rubber policeman. The sample was then centrifuged for 15 minutes and 3200 rpm, and the supernatant (~7 mL) removed and discarded. The vial was placed in the oven to dry for 12 hours at 60 ^{o}C and returned to the laboratory.

2.3.2 Distinct analytical procedures for VL1 samples

POC/PON analyses for the 0.8 µm size fraction collected by filtration were done by packing five 5 mm diameter aliquots (punches) of the 47 mm diameter GF/F filters into acid-resistant 5x8 mm silver cups (Sercon SC0037), treating these with two 20 µl aliquots of 2 N HCl to remove carbonates [*P King et al.*, 1998], and drying at 60 ^{o}C for at least 48 hours. For the 50 µm mesh filtration samples, and the centrifuge samples, 0.5-1.0 mg aliquots of the dried (72 hours at 60 ^{o}C) centrifuge pellet remaining after PIC coulometry were encapsulated in 4x6 mm silver cups (Sercon SC0036). Analyses of all these sample types was by catalytic combustion using a Thermo-Finnigan Flash 1112 elemental analyzer calibrated against sulphanilamide standards (Central Sciences Laboratory, University of Tasmania). Precision of the analysis was +/- 1 %. A blank correction for of 0.19 ± 0.09 ug C was applied which represented 1.6 % of an average sample.

PIC concentrations were determined for subsamples of the 0.8 μm GF/F filters (half of the filter), the whole 50 μm mesh screens, and the whole centrifuge samples by closed system acidification and coulometry using a UIC CM5011 CO_2 coulometer. The samples were placed in glass vials (or in the case of the centrifuge tubes connected via an adaptor), connected to a manual acidification unit and condenser and maintained at 40°C after acidification with 4mL of 1N HCl, and swept with a nitrogen gas-flow (~100 mL min^{-1}) via a drier and aerosol filter (Balston) into the coulometry cell. Calibration versus calcium carbonate standards (200 to 3000ug) provided precision of ± 0.3%. However, for the 0.8 μm filter, precision was limited to 10 % by sub-sampling of the filter due to uneven distribution. Blank corrections were applied to the 0.8 μm size fraction, being 2.4 ± 1.8 ug C representing 8.8 % of an average sample. The 50 μm fraction blank correction was 3.3 ± 0.1 ug C, representing 22 % of an average sample. Centrifuge pellet coulometry blank subtraction was 2.0 ± 0.1 ug C, equivalent to 2.8 % of an average sample.

Biogenic silica analysis of the residues remaining after PIC analysis of the centrifugation samples, was by alkaline digestion (0.2 N NaOH) in a 95°C water bath for 90 minutes, similar to the method described by Paasche (1973) and as described in section 2.2.2. with the variation that 4 mL of each sample was transfered from the centrifuge tubes and filtered using a syringe filter before dilution to 10mL.

2.3.3 Comparison of VL1 to other voyages

The first survey on VL1 in 2008 differed from later efforts in two important ways: i) POC and PIC samples were collected by both filtration and centrifugation, ii) separate BSi samples were not collected - instead BSi analyses were carried out only on the sample residues from PIC coulometric sample digestions of the centrifuge samples. Comparison of POC and PIC results from the centrifugation samples (effectively total samples without size fractionation) and the filtration samples (separated into the PIC01 0.8-50 μm and PIC50 50-1000 μm size fractions) shows (Figure 2) that filtration collected somewhat more PIC (order 20-30 %) and considerably more POC (order 200-300 %) than centrifugation. This fits with the possibility of loss of material from the continuous centrifuge cup, with greater loss of lower density organic matter (and possible additional loss of organic matter via dissolution in the ethanol rinsing step). Thus for comparison of VL1 POC and PIC to the other voyages we use only the filtration results, thereby avoiding methodological biases. For BSi, we do not have this possibility. Based on the low centrifuge yields for PIC and POC we can expect that the VL1 BSi values are also too low. This is confirmed by comparison to the other voyages which reveals that VL1 BSi values were lower than those of other voyages, especially in the far south where BSi values were generally highest (data shown below), but nonetheless had similar

north-south latitudinal trends. For this reason, our further interpretation of the VL1 BSi results is only in terms of these latitudinal trends.

2.4 Analysis of nutrients, DIC, alkalinity, and calculation of pH and calcite saturation

Nutrients were analysed onboard ship for VL1 to VL5, and on frozen samples returned to land for VL6-9, all by the CSIRO hydrochemistry group following WOCE/CLIVAR standard procedures, with minor variations [*Eriksen*, 1997], to achieve precisions of ~1% for nitrate, phosphate, and silicate concentrations. Dissolved inorganic carbon (DIC) and alkalinity samples were collected in gas tight bottles poisoned with mercuric chloride and measured at CSIRO by coulometry and open cell titration, respectively [*Dickson et al.*, 2007]. Comparison to certified reference materials suggests accuracy and precision for both DIC and alkalinity of better than ± 2 μmol kg^{-1}. Full details were recently published [*Roden et al.*, 2016]. Calculation of pH (free scale) and calcite saturation were based on the Seacarb version 3.1.2 software (https://CRAN.R-project.org/package=seacarb), which uses the default selection of equilibrium constants given in [*Van Heuven et al.*, 2011].

2.5 Satellite derived ocean properties and the NASA Ocean Biogeochemistry Model

The locations of oceanographic fronts in the Australian sector were estimated from satellite altimetry, following the approach of [*S. Sokolov and Rintoul*, 2002], updated as follows. Absolute sea surface height (SSH) was calculated by adding the sea surface height anomaly from AVISO+ [*Pujol et al.*, 2016] to the 2500 dbar reference level mean dynamic topography of [*Olbers et al.*, 1992]. The positions of the fronts were then identified using the sea surface height contours corresponding to the positions of the Southern Ocean fronts identified by [*S. Sokolov and Rintoul*, 2007a] in the region 100-180 °E. From this analysis, we show 8 fronts from north to south consisting of:
Fronts 1-3: north, middle, and south branches of the Subantarctic Front (SAF), which bound the highest velocity jets of the ACC. Fronts 4-6: north, middle, and south branches of the Polar Front (PF), associated with subsurface temperature features related to the strength of the ACC and with the shoaling of CDW in the overturning circulation. The Polar Frontal Zone (PFZ) lies between the northernmost of these branches and the SAF to its north. Fronts 7-8: north and south branches of the Southern Antarctic Circumpolar Current Front (sACCf) front, marking weaker flows in Antarctic waters of the ACC and occurring near where upwelling of old nutrient rich and relatively acidic Circumpolar Deep Water comes closest to the surface.

We do not show the Subtropical Front (STF) that marks the northern boundary of the Southern Ocean, or the Southern Boundary Front, which marks the southern edge of the ACC (separating it from westerly flow in Antarctic shelf waters). This is because both features have weak, discontinuous SSH signatures south of Australia: mesoscale eddies rather than the STF dominate the weak SSH field in the Subantarctic Zone (SAZ; between the STF and the SAF), and detection of the Southern Boundary

335 Front is confounded by proximity to the Antarctic shelf where altimetry is impacted by other
336 processes, including sea-ice cover for much of the year [*S. Sokolov and Rintoul*, 2007a].
337
338 We considered using these dynamic heights and front locations as ordinates for the spatial
339 distributions of POC, PIC and BSi. In the core of the ACC (50-60 °S), this did help explain some
340 departures from monotonic north-south trends as resulting from meanders of the fronts, but latitude
341 was more strongly correlated with PIC abundance in the SAZ and with BSi in southern ACC waters
342 and Antarctic shelf waters, where dynamic height contours were only weakly varying. Accordingly,
343 there was no overall advantage of replacing latitude by dynamic height as a predictor of biogenic
344 mineral concentrations, and we have used latitude as the ordinate in our figures and discussion.
345
346 Sea surface temperatures (°C) were obtained from the NASA MODIS Aqua 11 μm night-only L3m
347 product available on-line:
348 https://giovanni.gsfc.nasa.gov/giovanni/#service=TmAvMp&starttime=&endtime=&data=MODISA_
349 L3m_SST_2014_nsst&variableFacets=dataFieldMeasurement%3ASea%20Surface%20Temperature
350 %3B
351 We chose the night values to avoid shallow ephemeral structures arising from daytime solar heating.
352 We refer to these estimates simply as SST values.
353
354 Phytoplankton chlorophyll concentrations (Chl in mg m^{-3} = ug L^{-1}) were obtained from the NASA
355 MODIS Aqua L3m product available on-line:
356 https://giovanni.gsfc.nasa.gov/giovanni/#service=TmAvMp&starttime=&endtime=&data=MODISA_
357 L3m_CHL_2014_chlor_a&variableFacets=dataFieldMeasurement%3AChlorophyll%3B
358 The full citation for this data is:
359 NASA Goddard Space Flight Center, Ocean Ecology Laboratory, Ocean Biology Processing Group.
360 Moderate-resolution Imaging Spectroradiometer (MODIS) Aqua Chlorophyll Data; 2014
361 Reprocessing. NASA OB.DAAC, Greenbelt, MD, USA.
362 doi:10.5067/AQUA/MODIS/L3M/CHL/2014.
363 The algorithm relies on the blue/green reflectance ratio for Chl values above 0.2 ug L^{-1} and
364 incorporates stray light correction based on the difference between red and blue light reflectances at
365 lower Chl levels. This product has been suggested to underestimate chlorophyll in the Southern Ocean
366 south of Australia (Johnson et al., 2013), but has the advantage of ongoing ready availability. For this
367 reason, we use it only for context and not for any detailed comparisons to shipboard observations. We
368 refer to these estimates as SChl values.
369
370 Particulate inorganic carbonate concentrations (mol m^{-3}) based on backscatter magnitudes [*W M Balch*
371 *et al.*, 2005] were obtained from the NASA MODIS/AQUA ocean colour product available on-line:

https://oceancolor.gsfc.nasa.gov/cgi/l3/A20111212011151.L3m_MO_PIC_pic_9km.nc.png?sub=img
The full citation for this data is:
NASA Goddard Space Flight Center, Ocean Ecology Laboratory, Ocean Biology Processing Group. Moderate-resolution Imaging Spectroradiometer (MODIS) Aqua Particulate Inorganic Carbon Data; 2014 Reprocessing. NASA OB.DAAC, Greenbelt, MD, USA. doi: 10.5067/AQUA/MODIS/L3M/PIC/2014.
We refer to these estimates as SPIC values. The veracity of these estimates in the Southern Ocean remains an active area of research. PIC sampling in the Subantarctic South Atlantic found levels 2-3 times lower than the satellite estimates [*W M Balch et al.*, 2011], and the algorithm also produces surprisingly high estimates in Antarctic waters, where limited shipboard surveys suggest that coccolithophore abundances drop strongly (work summarized in Balch et al., 2005). Our data provides the most extensive PIC observations for comparison to SPIC values in Antarctic waters yet available, and is discussed in detail below. Comparison of PIC and SPIC values at individual sampling sites was based on combined data from MODIS Aqua and Terra 9km daily products. SPIC values were an average of pixels within 25 km of PIC sampling sites on the same day.

Modeled coccolithophore distributions were obtained from the data-assimilating general circulation model NASA Ocean Biogeochemical Model (NOBM) available on-line:
https://giovanni.gsfc.nasa.gov/giovanni/#service=TmAvMp&starttime=&endtime=&data=NOBM_MON_R2014_coc&variableFacets=dataFieldDiscipline%3AOcean%20Biology%3BdataFieldMeasurement%3APhytoplankton%3B
The phytoplankton function type model is based on [*Watson W Gregg and Casey*, 2007a]. Details of particular relevance to comparisons with our observations are discussed in section 3.4.

3. Results and Discussion

3.1 Representativeness of oceanographic sampling

As shown in Figure 1, sampling covered all Southern Ocean zones from sub-tropical waters in the north to seasonally sea-ice covered waters in the south (covering SST ranging from -1 to 23 °C). Almost all samples were representative of high-nutrient low-chlorophyll Southern Ocean waters, indicative of iron limitation. Exceptions occurred near Tasmania, where moderate levels of SChl were occasionally present, and over the Antarctic shelf where locally very high levels of SChl were present. Individual maps for each voyage leg of SChl are provided in the Supplementary Material and of satellite reflectance based estimates of PIC (SPIC) below, and reveal that higher values of SChl and SPIC are often associated with mesoscale structures, especially in the Subantarctic and Polar Frontal Zones. This means that mesoscale variability makes satellite versus shipboard comparisons difficult, and this problem is exacerbated by frequent cloud cover. Both techniques characterize the very upper

409 water column, with ship samples from ~4m depth and the satellite ocean colour observations
410 reflecting the e-folding penetration depth of ~10-15 m [*Grenier et al.*, 2015; *Morel and Maritorena*,
411 2001].
412
413 It appears likely that our single-depth sampling can be considered as representative of upper water
414 column phytoplankton concentrations, because pigment samples and profiles of beam attenuation and
415 night-time fluorescence from some of these voyages as well as previous work show that biomass is
416 generally well mixed in the upper water column, and that when subsurface chlorophyll maxima are
417 present they primarily reflect increased chlorophyll levels rather than increased phytoplankton
418 abundances [*Andrew R. Bowie et al.*, 2011a; *A.R. Bowie et al.*, 2011b; *Parslow et al.*, 2001; *Rintoul*
419 *and Trull*, 2001; *Shadwick et al.*, 2015; *Trull et al.*, 2001b; *S. W. Wright et al.*, 1996; *S.W. Wright and*
420 *van den Enden*, 2000]. This perspective is also consistent with the limited information on the depth
421 distributions of coccolithophores in the Southern Ocean, which generally exhibit relatively uniform
422 and maximal values (especially for the most abundant species, *Emiliania huxleyi*) within the surface
423 mixed layer [*Findlay and Giraudeau*, 2000; *Holligan et al.*, 2010; *Mohan et al.*, 2008; *Takahashi and*
424 *Okada*, 2000]. There is some evidence that this conclusion can also be applied to the PIC50
425 foraminiferal fraction, in that the most abundant of these organisms tend to co-locate with
426 phytoplankton in the mixed layer in the Southern Ocean [*Mortyn and Charles*, 2003].
427
428 **3.2 Latitudinal distributions of BSi, PIC, and POC**
429 All the Voyage Legs exhibited similar latitudinal variations of the measured chemical components
430 (Figure 3). BSi, predominantly derived from diatoms, was clearly the dominant biogenic mineral in
431 the south in Antarctic waters. PIC01 concentrations, predominantly derived from coccolithophores,
432 were highest in northern Subantarctic waters, although even there BSi was often present at similar
433 levels. Interestingly, PIC50 concentrations, predominantly derived from foraminifera, often exhibited
434 maxima in the middle of the Southern Ocean at latitudes of 55-60 °S. The latitudinal variations in all
435 these biogenic mineral concentrations were quite strong, exceeding two orders of magnitude. In
436 contrast, variations in POC were 10-fold smaller, and often quite uniform across the central Southern
437 Ocean, with maxima sometimes in the far north near Tasmania and sometimes in the far south over
438 the Antarctic shelf (Figure 3). Variations in BSi, PIC, and POC concentrations among the voyages, at
439 a given latitude, were smaller than these north-south trends. It seems likely that these smaller
440 variations were partly seasonal, in that the earliest seasonal voyage leg (VL4 in September) had lower
441 concentrations of every component. But across the other voyages, ranging from mid-November
442 (VL5) to mid-April (VL1) no clear seasonal cycle was exhibited, perhaps owing to variations in
443 sampling location, and the known importance of inter-annual and mesoscale structures in Southern
444 Ocean phytoplankton distributions (e.g. [*Moore et al.*, 1999; *Moore and Abbott*, 2002; *S. Sokolov and*
445 *Rintoul*, 2007b]). As noted in the Methods section (2.3), the BSi values for VL1 stand out as being too

low, in that they were well below those of other voyages, while the POC, PIC01, and PIC50 values were similar.

The latitudinal dependence of the relative importance of diatoms and coccolithophores is revealed by viewing the BSi/PIC01 ratios as an ensemble for all the voyages (use of the ratio helps to remove seasonal and interannual variations in their abundances which tend to track each other at a given latitude). The BSi/PIC01 ratio reaches values of 200 in the far south and decreases north of 50 °S to values near 1 (Figure 4a). Approximate equivalence of BSi and PIC01 occurs relatively far north in the Southern Ocean, near 50 °S, and thus near the southern edge of the Subantarctic Zone. This persistence of the importance of diatoms as a major component of the phytoplankton community in northern waters of the Southern Ocean must reflect the winter-time renewal of silica supply from upwelled deep waters in the Southern Ocean that are carried north by Ekman transport, combined with recycling of biogenic silica within surface waters, given that by mid-summer silicate is largely depleted north of the Subantarctic Front [*Nelson et al.*, 2001; *Trull et al.*, 2001b]. Accordingly the relative dominance of diatoms and coccolithophores in the SAZ may be quite sensitive to changes in the overturning circulation and westerly wind field. How this might translate into impacts on the biological carbon pump remains far from clear. Interestingly, deep ocean sediment traps in the SAZ south of Australia reveal strong dominance (4-fold) of PIC over BSi in the export flux to the ocean interior, reminding us that export can be selective (and also that foraminifera can contribute a significant fraction of total PIC, estimated to vary from ~1/3 to 2/3; [*A L King and Howard*, 2003]). The POC flux recovered by these deep sediment traps was close to the global median and similar to that of biogenic silica dominated fluxes in the Polar Frontal Zone to the south [*Trull et al.*, 2001a].

The importance of diatoms across the entire Southern Ocean, relative to coccolithophores is further emphasized by expressing their biogenic mineral abundances in terms of associated POC, using average values for the POC/BSi ratio of iron-limited diatoms (3.35, equivalent to a Si/N ratio of 2 and Redfield C/N ratio of 6.7 [*Olivier Ragueneau et al.*, 2006; *Takeda*, 1998]) and the POC/PIC ratio of coccolithophores (1.5, for *Emiliania huxleyi* morphotype A, the dominant Southern Ocean species, [*Bach et al.*, 2015; *M. N. Muller et al.*, 2015]). As shown in Figure 4b, this suggests that diatoms dominate the accumulation of organic carbon throughout the Southern Ocean, with coccolithophores generally contributing less than half that of diatoms in the SAZ and less than a tenth of that in Antarctic waters. This statement is of course limited to POC captured by our small volume, size limited (1-1000 mm), sampling procedure, and variability in the extent of dominance and the scaling of POC to biogenic minerals still allows significant contributions from other POC sources. The relatively small POC contribution from coccolithophores is only weakly sensitive to the ~3-fold variation [*M. N. Muller et al.*, 2015] of POC/PIC ratios among *Emiliania huxleyi* morphotypes. Using the lower value of 0.83 observed for over-calcified forms that occur in the northern SAZ would reduce the POC contribution

there but still leave it co-dominant with diatoms, and using the higher value of 2.5 observed for polar morphotype C would increase the POC contribution in Antarctic waters, but still leave it overwhelmed by the diatom contribution (Figure 4b). The relative contributions to total POC are also sensitive to the POC/BSi ratio chosen for diatoms (which vary significantly across genera; [*O. Ragueneau et al.*, 2002; *Olivier Ragueneau et al.*, 2006]). For these reasons, the relative dominance is best viewed on the log scale of Figure 4b, and while keeping in mind the considerable scatter.

Figure 4b also emphasizes that total POC contents can be largely explained by diatom biomass in Antarctic waters (south of 50 °S), whereas in the SAZ (north of 50 °S), total POC often exceeds the sum of contributions from diatoms and coccolithophores. This serves as an important reminder that other organisms are important to the carbon cycle in the SAZ, and phytoplankton functional type models should avoid over-emphasis on diatoms and coccolithophores just because they have discernable biogeochemical impacts (on silica and alkalinity, respectively) and satellite remote sensing signatures [*Hood et al.*, 2006; *Moore et al.*, 2002]. Finally, we note that the relatively low levels of PIC across the Southern Ocean as observed here means that POC/PIC ratios are high, greater than 4 in the SAZ and ranging up to 20 in Antarctic waters (Figure 4a). This suggests calcification has a negligible countering impact on the reduction of surface ocean CO_2 partial pressure by phytoplankton uptake, even smaller than the few to ~10% influence identified earlier from deep sediment trap compositions in HNLC [*P. W. Boyd and Trull*, 2007a] and iron-enriched waters, respectively [*Salter et al.*, 2014].

Notably, our Southern Ocean PIC01 estimates are smaller than those found in northern hemisphere polar waters. As compiled by Balch et al. (2005), concentrations were 100-fold higher (~10 μM) in the north Atlantic south of Iceland (60-63 °N) than any of our values, and 1000-fold higher than our values in the same southern hemisphere latitude range. Values collected over many years from the Gulf of Maine [*W M Balch et al.*, 2008] were ~ 1 μM, and thus 5-10 times higher than our SAZ values (Gulf of Maine summer temperatures are similar to the SAZ, and colder in winter). This difference between hemispheres is also evident in observations from the South Atlantic, where PIC values estimated from acid labile backscatter for 6 voyages between 2004 and 2008 and latitudes 40-50 °S were ~0.1-0.5 μM in remote waters [*W M Balch and Utgoff*, 2009], increasing to 1-2 μM in the Argentine Basin with a few values reaching 4 μM [*W Balch et al.*, 2014]. These high South Atlantic observations are the highest of the "Great Calcite Belt" identified as a circumpolar feature of Subantarctic waters based on SPIC values [*W Balch et al.*, 2014; *W M Balch et al.*, 2011]. Notably, shipboard PIC measurements in this feature are 2-3 times lower than the SPIC estimates in the South Atlantic [*W M Balch et al.*, 2011], and ship collected samples from two voyages across the South Atlantic and Indian sectors [*W M Balch et al.*, 2016] exhibit PIC concentrations (actual PIC values

519 accessed online at http://www.bco-dmo.org/dataset/560357, rather than the PIC estimates from acid-
520 labile backscatter shown in the paper) that decrease eastwards in this feature to reach values close to
521 our observations in the Australian sector of ~ 0.1 μM (Figure 3).
522
523 **3.3 Comparison to satellite PIC (SPIC) estimates**
524 As is very evident from the limited observations we have achieved from our efforts over many years,
525 it will never be possible to characterize Southern Ocean phytoplankton population dynamics from
526 ship based sampling – the influences of mesoscale circulation, ephemeral inputs of the limiting
527 nutrient iron, and food web dynamics produce variability that cannot be adequately assessed in this
528 way, leaving sparse sampling open to potentially large biases. Use of satellite observations is clearly
529 the path forward to alleviate this problem, and development of algorithms for global coccolithophore
530 distributions has been a major advance [*W M Balch et al.*, 2005; *Brown and Yoder*, 1994]. Until
531 recently the calibration of these SPIC values has been based primarily on North Atlantic observations.
532 Work to check these efforts for the Southern Ocean has begun, but remains sparse. Early work in the
533 South Atlantic found that SPIC values appeared to exceed ocean PIC by a factor of 2-3 [*W M Balch et*
534 *al.*, 2011], and based on a handful of samples it was suggested that this might reflect a lower amount
535 of PIC per coccolith [*Holligan et al.*, 2010], and it has since been confirmed that polar
536 coccolithophores can have low PIC contents [*Charalampopoulou et al.*, 2016; *M. N. Muller et al.*,
537 2015; *Poulton et al.*, 2011]. Two dedicated voyages to investigate the "Great Calcite Belt" in the SAZ
538 and PFZ across the South Atlantic and South Indian Oceans, attempted comparison of acid-labile
539 backscatter (as a proxy for PIC) and MODIS SPIC values, but there were no match-ups in the South
540 Atlantic owing to cloudy conditions [*W M Balch et al.*, 2016]. Results from the South Indian sector,
541 and from other voyages in the South Atlantic show high acid-labile backscatter which translates into
542 high SPIC estimates in the SAZ and PFZ (especially in naturally iron-fertilized waters), but also high
543 values further south which are not in agreement with ship observations [*W M Balch et al.*, 2016; *Smith*
544 *et al.*, 2017].
545
546 Comparison of our ship observations to MODIS SPIC estimates are shown in Figure 5 for each
547 voyage leg. These reveal some agreement in the SAZ in terms of identifying moderate levels of PIC,
548 often in association with higher levels of total SChl (Supplementary Material), but differ strongly in
549 Antarctic waters where all ship observations reveal low PIC values, whereas the SPIC estimates in
550 Antarctic waters reach and often exceed those in the SAZ, especially over the Antarctic shelf. Both
551 cloudy conditions and strong mesoscale variability limit the number of direct comparisons (match-
552 ups) that can be made. Using a match-up length scale of 25 km (i.e. the ship and satellite observations
553 must be within 25 km of each other on the same day), which is somewhat larger than the correlation
554 length scale for chlorophyll in the Southern Ocean of 10-15 km [*Haëntjens et al.*, 2017], allowed us to
555 retain 116 match-ups. These results, shown in Figure 6, confirm that the satellite SPIC values are

reasonable estimates in Subantarctic waters, within a factor of 2-3 [*W M Balch et al.*, 2011], but very much too high in Antarctic waters.

3.4 Comparison to possible environmental controls on coccolithophore growth rates

The ship observations provided here offer a significant advance in quantifying the distributions of coccolithophores in the Southern Ocean south of Australia, but much less understanding of why these distributions arise and therefore how they might change in response to climate, circulation, and biogeochemical changes in the future. Coccolithophores, especially the most common species *Emiliania huxleyi*, have been studied sufficiently in the laboratory to allow possible important controls on their niches and especially their calcification rates to be proposed, including temperature, pH, pCO_2, calcite saturation state, light, and macro- and micro-nutrient availability [*Bach et al.*, 2015; *Feng et al.*, 2016; *Mackinder et al.*, 2010; *M. N. Muller et al.*, 2015; *Müller et al.*, 2017; *Schlüter et al.*, 2014; *Schulz et al.*, 2007; *Sett et al.*, 2014; *Zhang et al.*, 2015]. We collected observations of many of these properties in parallel with our PIC observations, and now briefly examine whether they present correlations that might contribute to understanding why coccolithophores are found mainly in northern Subantarctic waters, and not further south. For illustrative purposes, we focus on VL3 (the mid- to late summer I9 northward hydrographic section from Antarctica to Perth) and VL6 (the early to mid-summer southward Astrolabe transit from Tasmania to Antarctica). VL3 covered the widest range of physical properties, and exhibited PIC01 concentrations that remained elevated further south than any other voyage (Figure 3). VL6 exhibited the more typical PIC01 distribution of a close to continuous decrease southward (Figure 3). The results from the other Voyage Legs were very similar to VL3 (figures not shown; data available in Supplementary Materials).

Many properties that might influence coccolithophore productivity decreased strongly and close to monotonically from north to south across the Southern Ocean for our voyages (Figure 7). These include temperature (from 23 to -0.4 C for our samples), salinity (from 35.6 to 33.6, with tight correlation with alkalinity, not shown - data available in the Supplementary Material), pH (from 8.20 to 8.08 on the free scale), and the saturation state of calcite (from 5.22 to 2.12). The strong correlation of these properties means that it is not easy to separate their possible influences on coccolithophore distributions, without relying on specific thresholds or quantitative response models. This problem of correlations among drivers has been noted before in examining transect data across Drake passage, where more detailed measurements of coccolithophore properties augmented with incubation studies found temperature and light were the most probable drivers of coccolithophore abundance and calcification rates [*Charalampopoulou et al.*, 2016]. Our lack of information on the availability of light (mixed layer depth was determined only on the two hydrographic sections), iron, or individual species and strains, makes deducing a possible influence of ocean acidification on coccolithophore

592 distributions from our spatial distribution data even more difficult. Nonetheless, we offer a few
593 pertinent observations. Firstly, the change in PIC01 abundances with latitude is much larger than
594 expected from models of the responses of calcification rates (normalized to maximum rates) to
595 inorganic carbon system variations (Figure 7). Two models are shown:
596
597 1. The "Bach model" based on independent terms for sensitivity to bicarbonate, CO_2, and pH. It
598 fits quite well the results from many laboratory incubations of *Emiliania huxleyi* strains under
599 conditions of modern and elevated pCO_2 [*Bach et al.*, 2015], and we have used values for the
600 constants (a, b, c, d) obtained from incubations of a strain isolated from Subantarctic waters
601 south of Tasmania [*Müller et al.*, 2017] to provide what might be considered the best current
602 model for the calcification rate response to changing inorganic carbon abundance and
603 speciation, following Eq. (1):
604
605 $$\text{Bach relative calcification rate} = a\,[HCO_3^-] / (b+[HCO_3^-]) - e^{-c[CO2]} - d[H^+] \quad (1)$$
606
607 2. The "Langdon model" based on a simple, inorganic precipitation motivated parameterization
608 of calcification as a function of calcite saturation state Ω [*Gattuso et al.*, 1998; *Langdon et al.*,
609 2000], which has been shown to apply in an approximate way to many corals [*Anthony et al.*,
610 2011; *Silverman et al.*, 2007], and perhaps to Southern Ocean foraminifera [*Moy et al.*, 2009].
611 We have chosen the simple linear form (n=1) and a sensitivity at the top end of the observed
612 range (a =1/4, so that calcification rate varies linearly from 0 to 1 for Ω=1 to 4), following Eq.
613 (2):
614
615 $$\text{Langdon relative calcification rate} = a\,(\Omega-1)^n \quad (2)$$
616
617 As shown in Figure 7, both these calcification rate models exhibit limited variations with latitude in
618 the Southern Ocean. The Bach model suggests negligible change in calcification rate. This is
619 essentially because the Southern Ocean variations in bicarbonate, CO_2, and pH are very small
620 compared to the future expected values used in incubation experiments. In addition, southward
621 cooling causes pH to rise, offsetting the impact of southward decrease in salinity and alkalinity, thus
622 reducing the southward decrease of pH and the associated drop in modeled calcification rate. The
623 Langdon model suggests approximately 3-fold decrease in calcification rate, which is considerably
624 smaller than the more than 10-fold drop in PIC01 (shown on a linear scale in Figure 7 and a
625 logarithmic scale in Figure 3). The shape of the Langdon model decrease shows some agreement with
626 that of PIC01 for VL6, but none for VL3 (which exhibits relatively constant significant PIC01
627 concentrations in the 40-50 °S latitude range where the Langdon model shows a strong decrease in

628 calcification rate, and then a strong drop in PIC01 south of 60 °S where the Langdon model shows no
629 change). Thus, and unsurprisingly, coccolithophore abundances are clearly not controlled by
630 inorganic carbon chemistry alone. This perspective has been strongly emphasized previously,
631 including by Bach et al., (2015), who noted " …great care must be taken when correlating carbonate
632 chemistry with coccolithophore dispersal because this is by no means the only parameter controlling
633 it. Physical (e.g. temperature), other chemical (e.g. nutrient concentrations), or ecological (e.g. grazing
634 pressure) factors will under many if not most circumstances outweigh the influence of carbonate
635 chemistry conditions…".
636
637 Many laboratory studies have emphasized the importance of temperature on coccolithophore growth
638 rates, as compiled recently [*Feng et al.*, 2016], and warming has been suggested as a possible cause of
639 decadal northward apparent range expansion in the North Atlantic [*Rivero-Calle et al.*, 2015] and the
640 occurrence of unusual blooms in the Bering Sea [*Merico et al.*, 2004]. To provide a brief visualization
641 of the expected univariate response, we fit the "Norberg" thermal optimum envelope model [*Norberg*,
642 2004] to growth rate data for 5-25 °C with modern pCO_2 and nutrient replete conditions for a
643 Southern Ocean morphotype A strain of *Emiliania huxleyi*, isolated from south of Tasmania [*M. N.*
644 *Muller et al.*, 2015], with optimum temperature z=15, thermal window w=10, and scaling constant *a*,
645 in which the exponential term represents the broad global temperature dependence of generic
646 phytoplankton growth rates [*Eppley*, 1972] and produces the known skewed form of organismic
647 thermal tolerances, following Eq. (3):
648
649 $$\text{Norberg growth rate } (d^{-1}) = a\,[1-((T-z)/w)^2]\,e^{0.0633T} \quad (3)$$
650
651 As shown in Figure 7, this predicts a drop from ~0.5 d^{-1} at the northern edge of the Southern Ocean to
652 zero growth near ~53 °S, whereas PIC01 concentrations fall off more slowly further south. The
653 presence of other morphotypes with lower thermal optima [*Cubillos et al.*, 2007] is an easy possible
654 way to explain this difference. Overall the Norberg temperature model has an advantage of the
655 calcification rate models – it does predict a strong decrease to negligible PIC01 values in the south.
656 There are of course many other possible explanations (as noted at the start of this section).
657
658 Interestingly, these uncertainties regarding the roles of inorganic carbon chemistry and temperature on
659 Southern Ocean coccolithophore distributions contrast with the possible role of macro-nutrients, in
660 that phosphate and nitrate increase southward across the Southern Ocean (e.g. [*Trull et al.*, 2001b]),
661 and were everywhere abundant during our surveys (nitrate > 3 μM , with phosphate/nitrate close to
662 Redfield expectations, data in Supplementary Material), and thus would be expected to lead to
663 southward increases in coccolithophore abundances which were not observed. For this reason we
664 suggest nitrate and phosphate availability is not an obvious driver of the southward decrease in

coccolithophore abundances in Southern Ocean HNLC waters (i.e. these nutrients are sufficient everywhere), although these nutrients may be important in determining the success of coccolithophores in oligotrophic waters at the northern edge of the Southern ocean, given the high half-saturation constant for nitrate uptake observed in some laboratory studies (~13 μM ; [*Feng et al.*, 2016]), and the possibility that high temperature and low nutrient conditions may non-linearly amplify phytoplankton stresses [*Thomas et al.*, 2017].

Importantly, in addition to multivariate environmental control of coccolithophore distributions via their growth rates, there is the possibility of control by resource competition with other autotrophs (presumably mainly for iron) and/or stronger loss terms to grazers in Antarctic than Subantarctic waters ([*Assmy et al.*, 2013] has suggested preferential grazing as a control on community structure; but we have no data to allow us to evaluate this). These are difficult issues to evaluate, and we provide just one comment. Diatom abundances as estimated from BSi concentrations show a stronger latitudinal relationship to silicon availability than coccolithophores do to carbonate availability (Figure 7). Diatoms abundances drop strongly near the SAF, north of which summer time $Si(OH)_4$ concentrations drop below 1 μM , i.e. close to the 'residual" concentration which it appears diatoms cannot access [*Paasche*, 1973]. Surveys of coccolithophores and diatoms in the SAZ in the South Atlantic and South Indian sectors have previously suggested that coccolithophore distributions may be linked to competition with diatoms [*W M Balch et al.*, 2016; *Smith et al.*, 2017], and this view is compatible with our observations, although it remains unproven. Further progress in understanding the controls on coccolithophore abundances in the Southern Ocean is clearly needed. At present temperature, light, and competition with diatoms for iron appear to be the strongest candidates (at least for southward expansion [*Charalampopoulou et al.*, 2016; *Gafar et al.*, 2017]; with nitrate a strong influence on the location of the northern oligotrophic boundary; [*Feng et al.*, 2016]).

3.5 Comparison to the NASA Ocean Biogeochemical Model

Many of these ideas about the roles of environmental conditions and ecological competition have been included in models for global coccolithophore distributions, e.g. [*Watson W Gregg and Casey*, 2007a; *Le Quere et al.*, 2005]; and we provide a brief comparison to one model – the NASA Ocean Biogeochemical Model (NOBM) for which simulation results are available on-line (see the Methods section). In brief, the NOBM predicts coccolithophore abundances (in Chl units) that are restricted to the far northern reaches of the Southern Ocean (Figure 8). This is also true for the Dynamic Green Ocean Model [*Le Quere et al.*, 2005]. This contrasts with our PIC results (Figures 3, 4, 7) and with PIC and coccolithophore cell counts from other sampling efforts which have found coccolithophore abundances to extend with similar concentrations right across the SAZ and sometimes the PFZ, e.g. during VL6 south of western Australia (Figures 3 and 7), south of Tasmania [*Cubillos et al.*, 2007],

in the Scotia Sea [*Holligan et al.*, 2010], and in the South Atlantic and South Indian Oceans, especially in regions of natural iron fertilization [*W M Balch et al.*, 2016; *Smith et al.*, 2017]. In the NOBM, diatoms are also simulated and show (Figure 8) the expected high abundance in Antarctic waters in the southern third of the Southern Ocean, decreasing northward as in our results (but also show a band of elevated diatom concentrations in the Subantarctic, which we did not observe).

Competition for nutrients in the NOBM favours the ability of coccolithophores over diatoms to get by on limited resources (half-saturation constants for nitrate and iron of 0.5 and 0.67 versus 1.0 and 1.0 μM) including light (half saturation constant of 56 versus 90 μmol photons m^{-2} s^{-1} under Southern Ocean low light conditions). But diatoms are specified to have higher growth rates when all resources are non-limiting (maximum growth rate at 20 °C 1.50 versus 1.13, both with the same Eppley dependence on temperature). Thus in the model, diatoms dominate silicon replete Southern Ocean waters, outcompeting other species for the limiting iron, and only give way to other species when silicon is depleted. Notably these other species then do best when additional Fe is supplied from either atmospheric sources (in the north where continental dusts are not shielded by ice) or island oases such as Crozet or Kerguelen. This view is compatible with our observations and those carried out in the northern half of the Southern Ocean during the "Great Calcite Belt" voyages [*W M Balch et al.*, 2016; *Smith et al.*, 2017]. It suggests that potential expansion of coccolithophores southward might be linked to decreasing supply of silicon from reduced upwelling of Circumpolar Deep Water in a progressively more stratified global ocean. A cautionary note to this conclusion is provided by the NOBM simulation of significant concentrations of diatoms in the SAZ where silicon is low, which arises from their specified higher maximum growth rate, emphasizing the importance of this parameter, and its temperature dependence, in modeling phytoplankton distributions. In specifying this temperature dependence, this model and most others still rely on the global compilation from nearly 50 years ago [*Eppley*, 1972]. Clearly better understanding of the controls on maximum growth rates and their temperature tolerance for key phytoplankton taxa is needed, first to understand current distributions and then to explore possible future changes.

4. Conclusions

Our surveys of PIC concentrations as a proxy for coccolithophores in the Southern Ocean south of Australia suggest:

- The concentrations of coccolithophores were much smaller (at least 10-fold) in the open Southern Ocean south of Australia than in northern hemisphere oceans.

- Coccolithophores were most abundant in the SAZ, and occasionally in the PFZ.

- The contribution of coccolithophores to total phytoplankton biomass (estimated from POC) was small, less than 10% in Subantarctic waters and less than 1% in Antarctic waters.

- The "Great Calcite Belt" characterization of SAZ and PFZ waters is overstated south of Australia, because both the satellite (SPIC) estimates and our in-situ PIC measurements show lower values than in the South Atlantic and South Indian where this feature was first suggested.
- The satellite PIC (SPIC) algorithm provides a good estimate, within a factor of 2-3, of PIC values in Subantarctic waters south of Australia, but erroneously suggests large agglomerations of PIC in polar waters, where little to none is present south of Australia.

- Our PIC results and ancillary measurements of biogenic silica, particulate organic carbon, dissolved nutrients, and inorganic carbon system status may be useful in the testing of models of limiting conditions and ecological competitions that affect coccolithophore distributions. Preliminary considerations suggest that temperature, iron, and competition with diatoms may be stronger influences than pH or calcite saturation state.

Despite the considerable effort required to obtain these survey results, much remains to be done just to define coccolithophore distributions, for example their seasonality, especially when the complexities of differing responses of individual species and strains are considered.

Acknowledgements

We thank Steve Rintoul (CSIRO Oceans and Atmosphere, Hobart) and Alain Poisson (Universite Pierre et Marie Curie, Paris) for allowing sample collection to proceed under the auspices of their science programs onboard *Aurora Australis* and *l'Astrolabe*, respectively. ACE CRC staff, students, and volunteers carried out onboard sampling, including Erik van Ooijen, Isobel Thomas, Peter Jansen, Stephane Thannassekos, and Nick Roden. Nutrient analyses were carried out by the CSIRO hydrochemistry group. Thomas Rodemann at the UTAS Central Sciences Laboratory did the CHN analyses. Funding was provided by the Australian Commonwealth Cooperative Research Centre Program via the ACE CRC. Tim Smit participated in the first voyage in 2008 and described those results in his Utrecht University Master thesis and in a poster presented at the Second Symposium on the Ocean in a High CO_2 World, Monoco, October 6-9, 2008. Andrew Lenton (CSIRO) produced the database of absolute mean dynamic heights. Our paper was significantly improved by insightful, constructive reviews from Alex Poulton and Lennart Bach.

References

Anthony, K., J. A Kleypas, and J. P. Gattuso (2011), Coral reefs modify their seawater carbon chemistry–implications for impacts of ocean acidification, *Global Change Biology*, *17*(12), 3655-3666.

Assmy, P., V. Smetacek, M. Montresor, C. Klaas, J. Henjes, V. H. Strass, J. M. Arrieta, U. Bathmann, G. M. Berg, and E. Breitbarth (2013), Thick-shelled, grazer-protected diatoms decouple ocean carbon and silicon cycles in the iron-limited Antarctic Circumpolar Current, *Proceedings of the National Academy of Sciences*, *110*(51), 20633-20638.

Bach, L. T., U. Riebesell, M. Gutowska, L. Federwisch, and K. G. Schulz (2015), A unifying concept of coccolithophore sensitivity to changing carbonate chemistry embedded in an ecological framework, *Progress in Oceanography*, *135*, 125-138.

Balch, W., D. Drapeau, B. Bowler, E. Lyczkowski, L. Lubelczyk, S. Painter, and A. Poulton (2014), Surface biological, chemical, and optical properties of the Patagonian Shelf coccolithophore bloom, the brightest waters of the Great Calcite Belt, *Limnol. Oceanogr*, *59*(5), 1715-1732.

Balch, W. M., N. R. Bates, P. J. Lam, B. S. Twining, S. Z. Rosengard, B. C. Bowler, D. T. Drapeau, R. Garley, L. C. Lubelczyk, and C. Mitchell (2016), Factors regulating the Great Calcite Belt in the Southern Ocean and its biogeochemical significance, *Global Biogeochemical Cycles*, *30*(8), 1124-1144.

Balch, W. M., D. T. Drapeau, B. C. Bowler, E. S. Booth, L. A. Windecker, and A. Ashe (2008), Space–time variability of carbon standing stocks and fixation rates in the Gulf of Maine, along the GNATS transect between Portland, ME, USA, and Yarmouth, Nova Scotia, Canada, *Journal of plankton research*, *30*(2), 119-139.

Balch, W. M., D. T. Drapeau, B. C. Bowler, E. Lyczskowski, E. S. Booth, and D. Alley (2011), The contribution of coccolithophores to the optical and inorganic carbon budgets during the Southern Ocean Gas Exchange Experiment: New evidence in support of the "Great Calcite Belt" hypothesis, *Journal of Geophysical Research*, *116*, C00F06, doi:10.1029/2011JC006941.

Balch, W. M., H. R. Gordon, B. C. Bowler, D. T. Drapeau, and E. S. Booth (2005), Calcium carbonate measurements in the surface global ocean based on Moderate-Resolution Imaging Spectroradiometer data, *Journal of Geophysical Research*, *110*, C07001; doi: 07010.01029/02004jc002560.

Balch, W. M., and P. E. Utgoff (2009), Potential interactions among ocean acidification, coccolithophores, and the optical properties of seawater, *Oceanography*, *22*(4), 146-159.

Be, A. W. H., and D. Tolderlund (1971), Distribution and ecology of living planktonic foraminifera in surface waters of the Atlantic and Indian Oceans, in *Micropaleontology of Oceans* edited by B. M. Funnel and W. R. Riedel, pp. 105-149, Cambridge University Press, New York.

Boeckel, B., K.-H. Baumann, R. Henrich, and H. Kinkel (2006), Coccolith distribution patterns in South Atlantic and Southern Ocean surface sediments in relation to environmental gradients, *Deep Sea Research Part I: Oceanographic Research Papers*, *53*(6), 1073-1099, doi:http://dx.doi.org/10.1016/j.dsr.2005.11.006.

Bowie, A. R., F. B. Griffiths, F. Dehairs, and T. W. Trull (2011a), Oceanography of the subantarctic and Polar Frontal Zones south of Australia during summer: Setting for the SAZ-Sense study, *Deep-Sea Research II*, *58*(21-22), 2059-2070, doi:10.1016/j.dsr2.2011.05.033.

Bowie, A. R., T. W. Trull, and F. Dehairs (2011b), Estimating the Sensitivity of the Subantarctic Zone to Environmental Change: the SAZ-Sense project., *Deep Sea Research II*, *58*(21-22), 2051-2058.

Boyd, P. W., and T. Trull (2007a), Understanding the export of biogenic particles in oceanic waters: Is there consensus?, *Progress in Oceanography*, *72*(4), 276-312, doi:10.1016/j.pocean.2006.10.007.

Boyd, P. W., and T. W. Trull (2007b), Understanding the export of marine biogenic particles: is there consensus?, *Progress in Oceanography*, *4*, 276-312, doi:210.1016/j.pocean.2006.1010.1007.

Brown, C. W., and J. A. Yoder (1994), Coccolithophore blooms in the global ocean,, *Journal of Geophysical Research*, *104C*, 1541-1558.

Buitenhuis, E., P. van der Wal, and H. J. W. de Baar (2001), Blooms of Emiliania huxleyi are sinks of atmospheric carbon dioxide: a field and mesocosm study derived simulation, *Global Biogeochemical Cycles*, *15*(3), 577-587.

Cao, L., and K. Caldeira (2008), Atmospheric CO2 stabilization and ocean acidification, *Geophysical Research Letters*, *35*(19), n/a-n/a, doi:10.1029/2008GL035072.

Charalampopoulou, A., A. J. Poulton, D. C. E. Bakker, M. I. Lucas, M. C. Stinchcombe, and T. Tyrrell (2016), Environmental drivers of coccolithophore abundance and calcification across Drake Passage (Southern Ocean), *Biogeosciences*, *13*(21), 5917-5935, doi:10.5194/bg-13-5917-2016.

Cubillos, J. C., S. W. Wright, G. Nash, M. F. d. Salas, B. Griffiths, B. Tilbrook, A. Poisson, and G. M. Hallegraeff (2007), Calcification morphotypes of the coccolithophorid Emiliania huxleyi in the Southern Ocean: changes in 2001 to 2006 compared to historical data, *Marine Ecology Progress Series*, *348*, 47-54, doi: 10.3354/meps07058.

Dickson, A. G., C. L. Sabine, and J. R. Christian (2007), Guide to Best Practices for Ocean CO2 Measurements*Rep.*, Sidney, British Columbia.

Doubleday, A. J., and R. R. Hopcroft (2015), Interannual patterns during spring and late summer of larvaceans and pteropods in the coastal Gulf of Alaska, and their relationship to pink salmon survival, *Journal of Plankton Research*, *37*(1), 134-150, doi:10.1093/plankt/fbu092.

Eppley, R. W. (1972), Temperature and phytoplankton growth in the sea, *Fisheries Bulletin*, *70*, 1063-1085.

Eriksen, R. (1997), A practical manual for the determination of salinity, dissolved oxygen, and nutrients in seawater*Rep. 11*, 83 pp, Hobart, Tasmania, Australia.

Eynaud, F., J. Giraudeau, J. J. Pichon, and C. J. Pudsey (1999), Sea-surface distribution of coccolithophores, diatoms, silicoflagellates and dinoflagellates in the South Atlantic Ocean during the late austral summer 1995, *Deep Sea Research Part I: Oceanographic Research Papers*, *46*(3), 451-482, doi:http://dx.doi.org/10.1016/S0967-0637(98)00079-X.

Feng, Y., M. Y. Roleda, E. Armstrong, P. W. Boyd, and C. L. Hurd (2016), Environmental controls on the growth, photosynthetic and calcification rates of a Southern Hemisphere strain of the coccolithophore Emiliania huxleyi, *Limnology and Oceanography*, *62*, 519-540, doi:10.1002/lno.10442.

Findlay, C. S., and J. Giraudeau (2000), Extant calcareous nannoplankton in the Australian Sector of the Southern Ocean (austral summers 1994 and 1995), *Marine Micropaleontology*, *40*(4), 417-439, doi:http://dx.doi.org/10.1016/S0377-8398(00)00046-3.

Gafar, N. A., B. D. Eyre, and K. G. Shulz (2017), A conceptual model for projecting coccolithophorid growth, calcification, and photosynthetic carbon fixation rates in response to global change (carbonate chemistry speciation, temperature, and light) based on *Gephyrocapsa oceanica*, *Frontiers in Marine Science*, *in review*.

Gattuso, J.-P., M. Frankignoulle, I. Bourge, S. Romaine, and R. Buddemeier (1998), Effect of calcium carbonate saturation of seawater on coral calcification, *Global and Planetary Change*, *18*(1), 37-46.

Gravalosa, J. M., J.-A. Flores, F. J. Sierro, and R. Gersonde (2008), Sea surface distribution of coccolithophores in the eastern Pacific sector of the Southern Ocean (Bellingshausen and Amundsen Seas) during the late austral summer of 2001, *Marine Micropaleontology*, *69*(1), 16-25, doi:http://dx.doi.org/10.1016/j.marmicro.2007.11.006.

Gregg, W. W., and N. W. Casey (2007a), Modeling coccolithophores in the global oceans, *Deep Sea Research Part II: Topical Studies in Oceanography*, *54*(5), 447-477.

Gregg, W. W., and N. W. Casey (2007b), Modeling coccolithophores in the global oceans, *Deep Sea Research Part II: Topical Studies in Oceanography*, *54*(5–7), 447-477, doi:http://dx.doi.org/10.1016/j.dsr2.2006.12.007.

Grenier, M., A. Della Penna, and T. W. Trull (2015), Autonomous profiling float observations of the high biomass plume downstream of the Kerguelen plateau in the Southern Ocean, *Biogeosciences 12*, 1–29, doi:10.5194/bg-12-1-2015.

Haëntjens, N., E. Boss, and L. D. Talley (2017), Revisiting Ocean Color algorithms for chlorophyll a and particulate organic carbon in the Southern Ocean using biogeochemical floats, *Journal of Geophysical Research: Oceans*, *122*(8), 6583-6593, doi:10.1002/2017JC012844.

Holligan, P., A. Charalampopoulou, and R. Hutson (2010), Seasonal distributions of the coccolithophore, Emiliania huxleyi, and of particulate inorganic carbon in surface waters of the Scotia Sea, *Journal of Marine Systems*, *82*(4), 195-205.

Hood, R. R., E. A. Laws, R. A. Armstrong, N. R. Bates, C. W. Brown, C. A. Carlson, F. Chai, S. C. Doney, P. G. Falkowski, and R. A. Feely (2006), Pelagic functional group modeling: Progress, challenges and prospects, *Deep Sea Research Part II: Topical Studies in Oceanography*, *53*(5), 459-512.

Kimball Jr, J., and E. Ferguson Wood (1964), A simple centrifuge for phytoplankton studies, *Bulletin of Marine Science*, *14*(4), 539-544.

King, A. L., and W. R. Howard (2003), Planktonic foraminiferal flux seasonality in Subantarctic sediment traps: A test for paleoclimate reconstructions, *Paleooceanography*, *18*(1), 1019, doi:1010.1029/2002PA000839, 002003.

King, P., H. Kennedy, P. P. Newton, T. D. Jickells, T. Brand, S. Calvert, G. Cauwet, H. Etcheber, B. Head, and A. Khripounoff (1998), Analysis of total and organic carbon and total nitrogen in settling oceanic particles and a marine sediment: an interlaboratory comparison, *Marine Chemistry*, *60*(3), 203-216.

Klaas, C., and D. E. Archer (2002), Association of sinking organic matter with various types of mineral ballast in the deep sea: Implications for the rain ratio, *Global Biogeochemical Cycles*, *16*(4), doi:10.1029/2001GB001765.

Langdon, C., T. Takahashi, C. Sweeney, D. W. Chipman, and J. Goddard (2000), Effect of calcium carbonate saturation state on the calcification rate on an experimental coral reef, *Global Biogeochemical Cycles*, *14*(2), 613C-DIC, 615N-NO613 and 618O-NO613 639-654.

Le Quere, C., S. P. Harrison, I. Colin Prentice, E. T. Buitenhuis, O. Aumont, L. Bopp, H. Claustre, L. Cotrim Da Cunha, R. Geider, and X. Giraud (2005), Ecosystem dynamics based on plankton functional types for global ocean biogeochemistry models, *Global Change Biology*, *11*(11), 2016-2040.

Mackinder, L., G. Wheeler, D. Schroeder, U. Riebesell, and C. Brownlee (2010), Molecular mechanisms underlying calcification in coccolithophores, *Geomicrobiology Journal*, *27*(6), 585-595.

McNeil, B. I., and R. J. Matear (2008), Southern Ocean acidification: A tipping point at 450-ppm atmospheric CO2, *Proceedings of the National Academy of Sciences 105*(48), 18860-18864, doi: 18810.11073/pnas.0806318105.

Merico, A., T. Tyrrell, E. J. Lessard, T. Oguz, P. J. Stabeno, S. I. Zeeman, and T. E. Whitledge (2004), Modelling phytoplankton succession on the Bering Sea shelf: role of climate influences and trophic interactions in generating Emiliania huxleyi blooms 1997–2000, *Deep Sea Research I*, *51*(12), 1803-1826, doi:1810.1016/j.dsr.2004.1807.1003.

Mohan, R., L. P. Mergulhao, M. V. S. Guptha, A. Rajakumar, M. Thamban, N. AnilKumar, M. Sudhakar, and R. Ravindra (2008), Ecology of coccolithophores in the Indian sector of the Southern Ocean, *Marine Micropaleontology*, *67*(1–2), 30-45, doi:http://dx.doi.org/10.1016/j.marmicro.2007.08.005.

Moore, J. K., M. R. Abbot, J. G. Richman, W. O. Smith, T. J. Cowles, K. H. Coale, G. W.D., and R. T. Barber (1999), SeaWiFS satellite ocean color data from the Southern Ocean, *Gephysical Research Letters*, *26*(10), 1465-1468.

Moore, J. K., and M. R. Abbott (2002), Surface chlorophyll concentrations in relation to the Antarctic Polar Front: seasonal and spatial patterns from satellite observations, *Journal of Marine Systems*, *37*, 69-86.

Moore, J. K., S. C. Doney, J. A. Kleypas, D. M. Glover, and I. Y. Fung (2002), An intermediate complexity marine ecosystem model for the global domain, *Deep-Sea Research II*, *49*, 403-462?

Morel, A., and S. Maritorena (2001), Bio-optical properties of oceanic waters- A reappraisal, *Journal of Geophysical research*, *106*(C4), 7163-7180.

Mortyn, P. G., and C. D. Charles (2003), Planktonic foraminiferal depth habitat and δ18O calibrations: Plankton tow results from the Atlantic sector of the Southern Ocean, *Paleoceanography*, *18*(2).

Moy, A. D., W. Howard, S. G. Bray, and T. Trull (2009), Reduced calcification in modern Southern Ocean planktonic foraminifera, *Nature Geoscience*, *2*(April), 276-280, doi:10.1038/NGEO460.

Muller, M. N., T. Trull, and G. M. Hallegraeff (2015), Differing responses of three Southern Ocean Emiliania huxleyi ecotypes to changing seawater carbonate chemistry, *Marine Ecology Progress Series*, *531*, 81-90, doi:10.3354/meps11309.

949 Muller, M. N., T. W. Trull, and G. Hallegraeff (2017), Independence of nutrient limitation
950 and carbon dioxide impacts on Southern Ocean coccolithophore Emiliania huxleyi, *Nature*
951 *- Microbial Ecology*, *in press*
952 Müller, M. N., T. W. Trull, and G. M. Hallegraeff (2017), Independence of nutrient limitation
953 and carbon dioxide impacts on the Southern Ocean coccolithophore Emiliania huxleyi,
954 *The ISME Journal*, 1-11, doi:10.1038/ismej.2017.53.
955 Nelson, D. M., M. A. Brzezinski, D. E. Sigmon, and V. M. Frank (2001), A seasonal
956 progression of Si limitation in the Pacific sector of the Southern Ocean, *Deep-Sea*
957 *Research II*, *48*, 3973-3995.
958 Norberg, J. (2004), Biodiversity and ecosystem functioning: a complex adaptive systems
959 approach, *Limnology and Oceanography*, *49*(4part2), 1269-1277.
960 Olbers, D. J., V. Gouretski, and G. S. J. Schroter (1992), *Hydrographic Atlas of the Southern*
961 *Ocean*, 99 pp., Alfred Wegener Institute for Polar and Marine Research, Bremerhaven.
962 Orr, J. C., et al. (2005), Anthropogenic ocean acidification over the twenty-first century and
963 its impact on calcifying organisms, *Nature 437*, 681-686, doi:610.1038/nature04095.
964 Paasche, E. (1973), Silicon and the ecology of marine plankton diatoms. I. Thalassiosira
965 pseudonana (Cyclotella nana) grown in a chemostat with silicate as limiting nutrient,
966 *Marine biology*, *19*(2), 117-126.
967 Parslow, J., P. Boyd, S. R. Rintoul, and F. B. Griffiths (2001), A persistent sub-surface
968 chlorophyll maximum in the Polar Frontal Zone south of Australia: seasonal progression
969 and implications for phytoplankton-light-nutrient interactions, *Journal of Geophysical*
970 *Research*, *106*, 31543-31557.
971 Pörtner, H. O., M. Langenbuch, and B. Michaelidis (2005), Synergistic effects of temperature
972 extremes, hypoxia, and increases in CO2 on marine animals: From Earth history to global
973 change, *Journal of Geophysical Research, Oceans*, *110*, doi:10.1029/2004JC002561.
974 Poulton, A. J., S. C. Painter, J. R. Young, N. R. Bates, B. Bowler, D. Drapeau, E.
975 Lyczsckowski, and W. M. Balch (2013), The 2008 Emiliania huxleyi bloom along the
976 Patagonian Shelf: Ecology, biogeochemistry, and cellular calcification, *Global*
977 *Biogeochemical Cycles*, *27*(4), 1023-1033.
978 Poulton, A. J., J. R. Young, N. R. Bates, and W. M. Balch (2011), Biometry of detached
979 Emiliania huxleyi coccoliths along the Patagonian Shelf, *Marine Ecology Progress Series*,
980 *443*, 1-17.
981 Pujol, M.-I., Y. Faugère, G. Taburet, S. Dupuy, C. Pelloquin, M. Ablain, and N. Picot (2016),
982 DUACS DT2014: the new multi-mission altimeter data set reprocessed over 20 years,
983 *Ocean Science*, *12*(5), 1067-1090.
984 Ragueneau, O., N. Dittert, P. Pondaven, P. Treguer, and L. Corrin (2002), Si/C decoupling in
985 the world ocean: is the Southern Ocean different?, *Deep-Sea Research II*, *49*, 3127-3154.
986 Ragueneau, O., S. Schultes, K. Bidle, P. Claquin, and B. Moriceau (2006), Si and C
987 interactions in the world ocean: Importance of ecological processes and implications for
988 the role of diatoms in the biological pump, *Global Biogeochemical Cycles*, *20*(4),
989 GB4S02.
990 Ridgwell, A., D. N. Schmidt, C. Turley, C. Brownlee, M. T. Maldonado, P. Tortell, and J. R.
991 Young (2009), From laboratory manipulations to Earth system models: scaling
992 calcification impacts of ocean acidification, *Biogeosciences*, *6*, 2611–2623.
993 Rintoul, S. R., and T. Trull (2001), Seasonal evolution of the mixed layer in the Subantarctic
994 Zone south of Australia, *Journal of Geophysical Research*, *106*(C12), 31447-31462,
995 doi:10.1029/2000JC000329.
996 Rivero-Calle, S., A. Gnanadesikan, C. E. Del Castillo, W. M. Balch, and S. D. Guikema
997 (2015), Multidecadal increase in North Atlantic coccolithophores and the potential role of
998 rising CO2, *Science*, *350*(6267), 1533-1537.

Roberts, D., W. R. Howard, J. L. Roberts, S. G. Bray, A. D. Moy, T. Trull, and R. R. Hopcroft (2014), Diverse trends in shell weight of three Southern Ocean pteropod taxa collected with Polar Frontal Zone sediment traps from 1997 to 2007, *Polar Biology*, *37*(10), 1445-1458, doi:10.1007/s00300-014-1534-6.

Roden, N. P., B. Tilbrook, T. W. Trull, P. Virtue, and G. D. Williams (2016), Carbon cycling dynamics in the seasonal sea-ice zone of East Antarctica, *Journal of Geophysical Research: Oceans*, doi:10.1002/2016JC012008.

Rost, B., and U. Riebesell (2004), Coccolithophores and the biological pump: responses to environmental changes, in *Coccolithophores*, edited, pp. 99-125, Springer.

Salter, I., R. Schiebel, P. Ziveri, A. Movellan, R. Lampitt, and G. A. Wolff (2014), Carbonate counter pump stimulated by natural iron fertilization in the Polar Frontal Zone, *Nature Geosci*, *7*(12), 885-889, doi:10.1038/ngeo2285.

Schiebel, R. (2002), Planktic foraminiferal sedimentation and the marine calcite budget, *Global Biogeochemical Cycles*, *16*(4), 1065.

Schlüter, L., K. T. Lohbeck, M. A. Gutowska, J. P. Gröger, U. Riebesell, and T. B. Reusch (2014), Adaptation of a globally important coccolithophore to ocean warming and acidification, *Nature Climate Change*, *4*(11), 1024-1030.

Schulz, K. G., B. Rost, S. Burkhardt, U. Riebesell, S. Thoms, and D. Wolf-Gladrow (2007), The effect of iron availability on the regulation of inorganic carbon acquisition in the coccolithophore *Emiliania huxleyi* and the significance of cellular compartmentation for stable carbon isotope fractionation, *Geochimica et Cosmochimica Acta*, *71*(22), 5301-5312.

Sett, S., L. T. Bach, K. G. Schulz, S. Koch-Klavsen, M. Lebrato, and U. Riebesell (2014), Temperature modulates coccolithophorid sensitivity of growth, photosynthesis and calcification to increasing seawater pCO2, *PLoS One*, *9*(2), e88308.

Shadwick, E. H., B. Tilbook, N. Cassar, T. W. Trull, and S. R. Rintoul (2015), Summertime physical and biological controls on O2 and CO2 in the Australian Sector of the Southern Ocean, *Journal of Marine Systems*, *147*, 21-28, doi:10.1016/j.jmarsys.2013.12.008.

Shadwick, E. H., T. Trull, H. Thomas, and J. A. E. Gibson (2013), Vulnerability of Polar Oceans to Anthropogenic Acidification: Comparison of Arctic and Antarctic Seasonal Cycles, *Scientific Reports*, *3*(August), 1-7, doi:10.1038/srep02339.

Silverman, J., B. Lazar, and J. Erez (2007), Effect of aragonite saturation, temperature, and nutrients on the community calcification rate of a coral reef, *Journal of Geophysical Research: Oceans*, *112*(C5).

Smith, H. E., A. J. Poulton, R. Garley, J. Hopkins, L. C. Lubelczyk, D. T. Drapeau, S. Rauschenberg, B. S. Twining, N. R. Bates, and W. M. Balch (2017), The influence of environmental variability on the biogeography of coccolithophores and diatoms in the Great Calcite Belt, *Biogeoscience Discussions*, *in review*, doi:10.5194/bg-2017-5110.

Sokolov, S., and S. R. Rintoul (2002), Structure of Southern Ocean fronts at 140E, *Journal of Marine Systems*, *37*(1-3), 151-184.

Sokolov, S., and S. R. Rintoul (2007a), Multiple jets of the Antarctic Circumpolar Current south of Australia, *Journal of Physical Oceanography*, *37*, 1394-1412, doi:1310.1175/JPO3111.1391.

Sokolov, S., and S. R. Rintoul (2007b), On the relationship between fronts of the Antarctic Circumpolar Current and surface chlorophyll concentrations in the Southern Ocean, *J. Geophys. Res. – Oceans*, *112*(C07030), doi: 10.1029/2006JC004072.

Takahashi, K., and H. Okada (2000), Environmental control on the biogeography of modern coccolithophores in the southeastern Indian Ocean offshore of Western Australia, *Marine Micropaleontology*, *39*(1–4), 73-86, doi:http://dx.doi.org/10.1016/S0377-8398(00)00015-3.

Takeda, S. (1998), Influence of iron availability on nutrient consumption ratio of diatoms in oceanic waters, *Nature*, *393*, 774-777.
Thomas, M. K., M. Aranguren□Gassis, C. T. Kremer, M. R. Gould, K. Anderson, C. A. Klausmeier, and E. Litchman (2017), Temperature–nutrient interactions exacerbate sensitivity to warming in phytoplankton, *Global Change Biology*, doi:10.1111/gcb.13641.
Trull, T., S. G. Bray, S. J. Manganini, S. Honjo, and R. Francois (2001a), Moored sediment trap measurements of carbon export in the Subantarctic and Polar Frontal Zones of the Southern Ocean, south of Australia, *Journal of Geophysical Research*, *106*(C12), 31489-31509, doi:10.1029/2000JC000308.
Trull, T., S. R. Rintoul, M. Hadfield, and E. R. Abraham (2001b), Circulation and seasonal evolution of polar waters south of Australia: Implications for iron fertilization of the Southern Ocean, *Deep-Sea Research Part Ii-Topical Studies in Oceanography*, *48*(11-12), 2439-2466, doi:10.1016/s0967-0645(01)00003-0.
Van Heuven, S., D. Pierrot, J. Rae, E. Lewis, and D. Wallace (2011), MATLAB program developed for CO2 system calculations, ORNL/CDIAC-105b, Carbon Dioxide Inf, *Anal. Cent., Oak Ridge Natl. Lab., US DOE, Oak Ridge, Tenn*.
Wright, S. W., D. P. Thomas, H. J. Marchant, H. W. Higgins, M. D. Mackey, and D. J. Mackey (1996), Analysis of phytoplankton of the Australian sector of the Southern Ocean: comparisons of microscopy and size frequency data with interpretations of pigment HPLC data using the 'CHEMTAX' matrix factorisation program, *Marine Ecology Progress Series*, *144*, 285-298.
Wright, S. W., and R. L. van den Enden (2000), Phytoplankton community structure and stocks in the East Antarctic marginal ice zone (BROKE survey, Jan.-Mar.1996) determined by CHEMTAX analysis of HPLC pigment signatures, *Deep-Sea Research II*, *47*(12), 2363-2400.
Zhang, Y., L. T. Bach, K. G. Schulz, and U. Riebesell (2015), The modulating effect of light intensity on the response of the coccolithophore Gephyrocapsa oceanica to ocean acidification, *Limnology and Oceanography*, *60*(6), 2145-2157.

Figure Captions

1. Map of sample sites (dots) relative to major Southern Ocean fronts (lines) and satellite SST (means for productive months, October-March, over the sample collection period 2008-2014). Front abbreviations: SAF = Subantartic Front, PF = Polar Front, sACCf = Southern Antarctic Circumpolar Current Front, N = North, M= Middle, S= South.

2. Comparison of centrifugation versus filtration size-fraction results for Voyage Leg 1, a) centrifugation total POC versus filtration POC (0.8-50 μm fraction): b) centrifugation total PIC versus filtration PIC01 (0.8-50 μm) and PIC50 (50-1000 μm) fractions.

3. Latitudinal variations in POC, BSi, PIC50, PIC01 concentrations for each voyage leg. See Table 1 for Voyage Leg details and Figure 1 for sample sites.

4. Latitudinal variations in the dominance of diatoms versus coccolithophores and their contributions to total POC, for results combined from all voyages: a) BSi/PIC01 and POC/(PIC50+PIC01) ratios, b) Percent contributions to total POC attributable to diatoms (assuming POC/BSi=3.35) and coccolithophores (assuming POC/PIC01=0.833).

5. Maps comparing ship based distributions of coccolithophore PIC distributions (PIC01, coloured dots) with satellite PIC estimates (SPIC; background colours) for each voyage leg. The SPIC estimates are averages for the month preceding the start of each voyage leg. Contour lines indicate dynamic height determined frontal positions for the week preceding the each voyage leg (see Figure 1 for front nomenclature).

6. Comparison of satellite SPIC and ocean PIC concentrations for the 116 match-ups for which satellite SPIC estimates were available within 25 km of the ocean PIC sample sites, on the same day. Colours indicate sample latitudes and show that good correlation occurs in Subantarctic waters, but strong overestimation by the satellite technique in Antarctic waters.

7. Latitudinal environmental conditions for voyage leg VL3 (left panels) and voyage leg VL6 (right panels): a, b) T, S, pH (free scale), calcite saturation, c, d) PIC01, Bach and Langdon relative calcification rate (dimensionless) and Norberg growth rate (d^{-1}) models, e, f) BSi and $Si(OH)_4$ concentrations (μM).

8. Maps of NASA Ocean Biogeochemical Model results for coccolithophore and diatom distributionsResults are means for productive month, October-March for 2008-2012, the last year available on-line: a) diatoms, b) coccolithophores.

Table 1. Sample Collection

#	Voyage Name	Leg	Dates	PIC50[3]	PIC01[3]	POC & PON[3]	BSi[3]
VL1	AA2008_V6 (SR3)	North	28/03/2008–15/04/2008	57/0	59/0	59/0	59/0
VL2	AA2012_V3 (I9)	South	05/01/2012–20/01/2012[1]	4/16	4/16	9/25	7/22
VL3	AA2012_V3 (I9)	North	20/01/2012–09/02/2012	62/0	62/0	59/0	53/0
VL4	AA2012_VMS (SIPEXII)	South	13/09/2012–22/09/2012	0/20	0/19	0/24	0/24
VL5	AA2012_VMS (SIPEXII)	North	11/11/2012–15/11/2012	0/24	0/24	0/27	0/28
VL6	AL2013_R2 (Astrolabe)	South	10/01/2013–15/01/2013	0/25	0/25	0/23	0/25
VL7	AL2013_R2 (Astrolabe)	North	25/01/2013–30/01/2013	0/27	0/27	0/26	0/27
VL8	AA2014_V2 (Totten)	South	05/12/2014–11/12/2014	0/36	0/36	0/32	0/37
VL9	AA2014_V2 (Totten)	North	22/12/2014–24/01/2015[2]	6/44	6/44	8/27	8/39

[1] 18/01/2012-20/01/2012 east to west traverse from approximately 65^0 S 144^0 E to 65^0 S 113^0 E included in South leg, see Figure 1

[2] 22/12/2014-11/1/2015 west to east traverse from approximately 65^0 S 110^0 E to 65^0 S 140^0 E included in North leg, see Figure 1

[3] Numbers of samples collected on station / underway

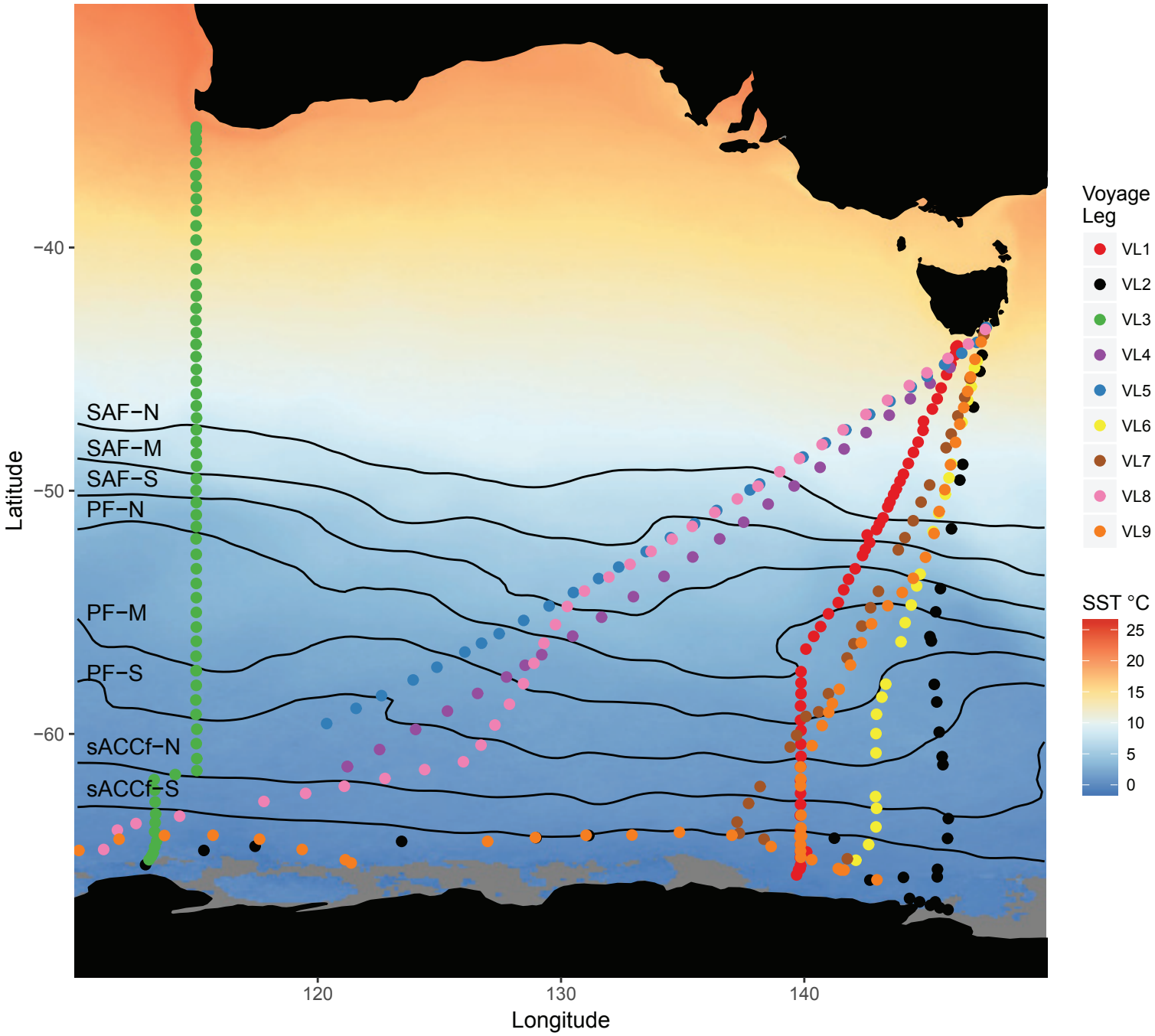
Latitude
−40
−50
−60
SAF−N
SAF−M
SAF−S
PF−N
PF−M
PF−S
sACCf−N
sACCf−S
120
130
140
Longitude
Voyage Leg
VL1
VL2
VL3
VL4
VL5
VL6
VL7
VL8
VL9
SST °C
25
20
15
10
5
0

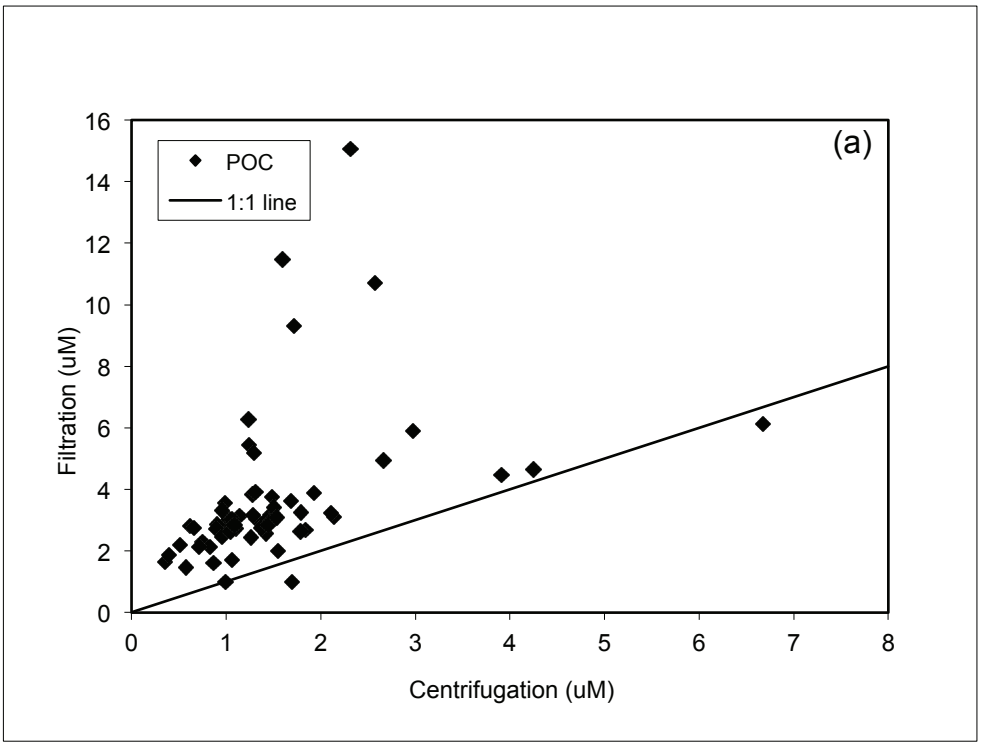
(a)
POC
1:1 line
Filtration (uM)
Centrifugation (uM)
0
2
4
6
8
10
12
14
16
0
1
2
3
4
5
6
7
8

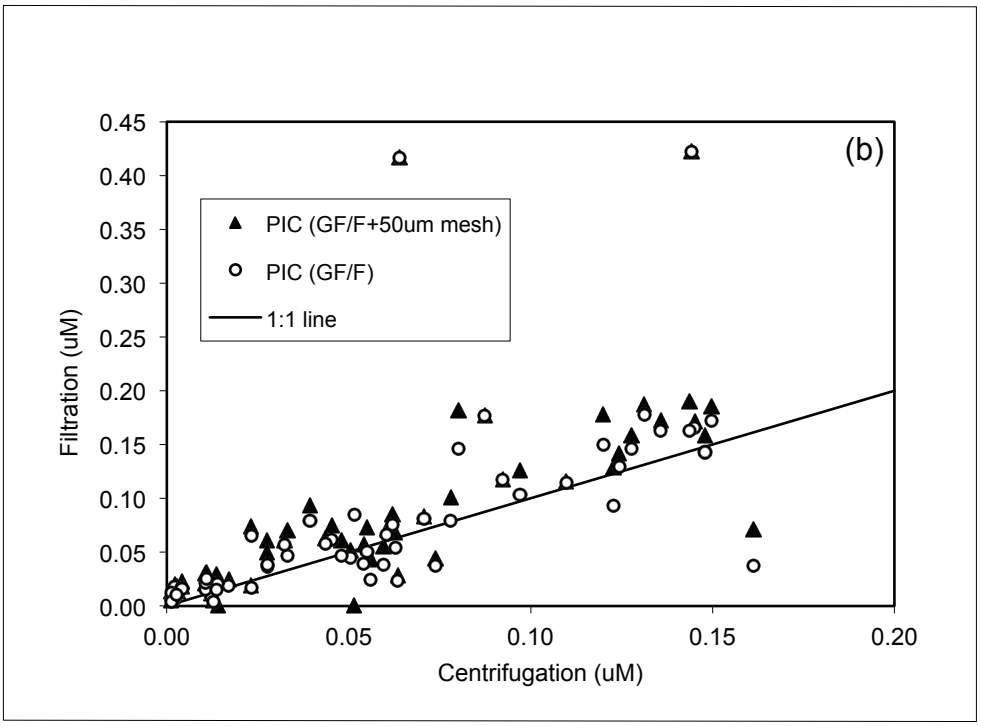
(b)
PIC (GF/F+50um mesh)
PIC (GF/F)
1:1 line
Filtration (uM)
Centrifugation (uM)
0.00
0.05
0.10
0.15
0.20
0.25
0.30
0.35
0.40
0.45
0.00
0.05
0.10
0.15
0.20

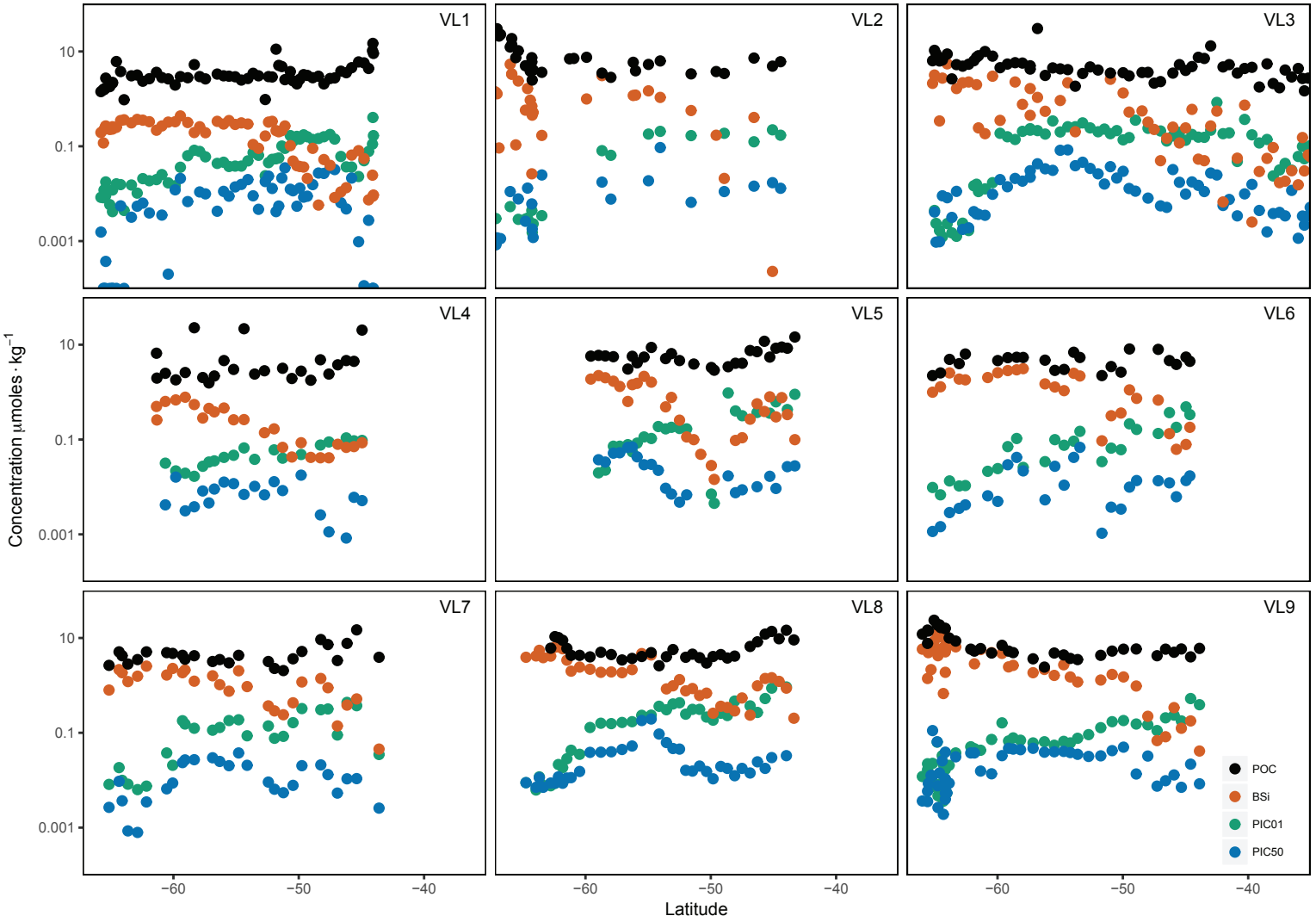
VL1
VL2
VL3
VL4
VL5
VL6
VL7
VL8
VL9
10
0.1
0.001
Concentration µmoles · kg^{-1}
−60
−50
−40
Latitude
POC
BSi
PIC01
PIC50

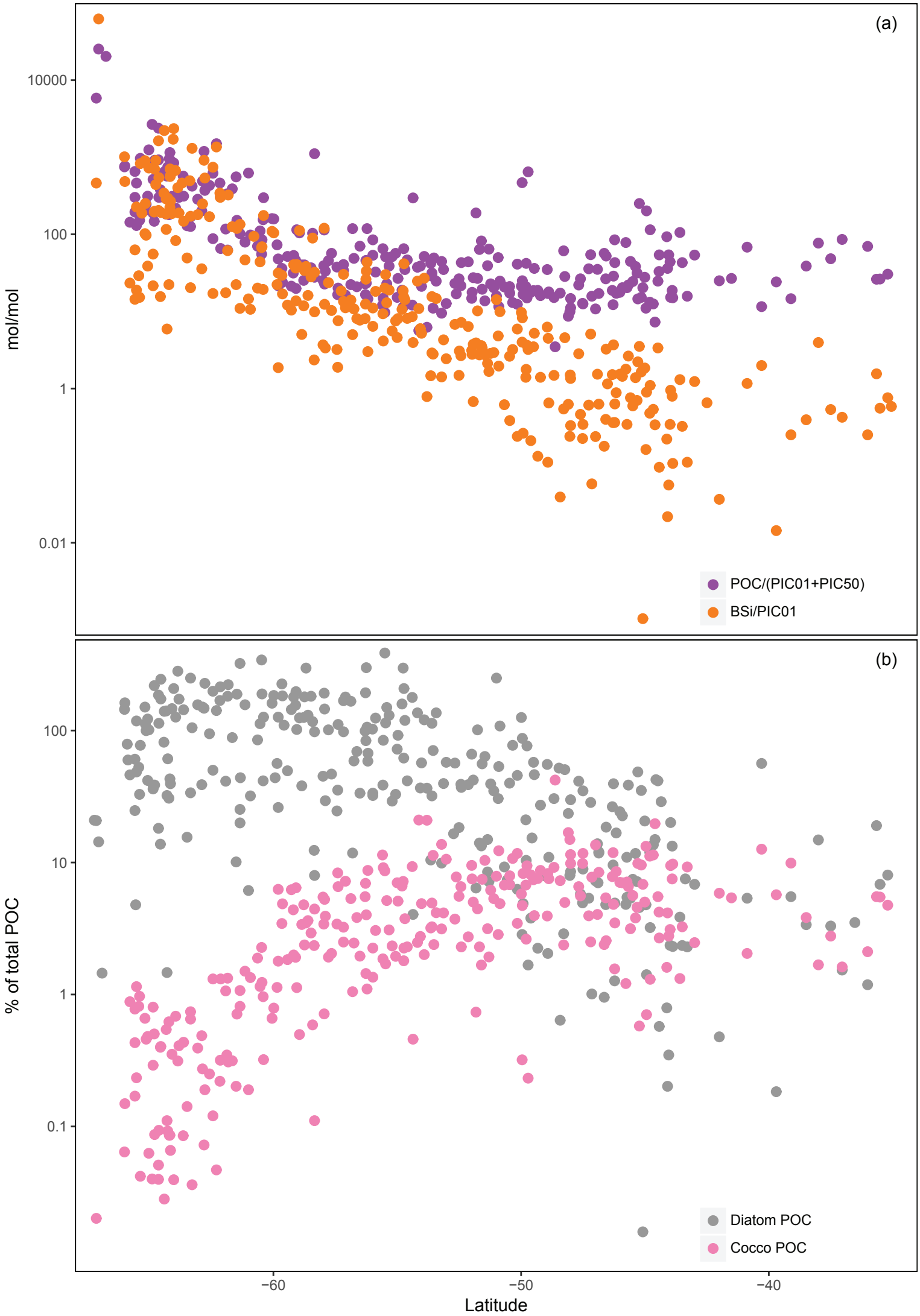
(a)
10000
100
1
0.01
mol/mol
POC/(PIC01+PIC50)
BSi/PIC01
(b)
100
10
1
0.1
% of total POC
Diatom POC
Cocco POC
−60
−50
−40
Latitude

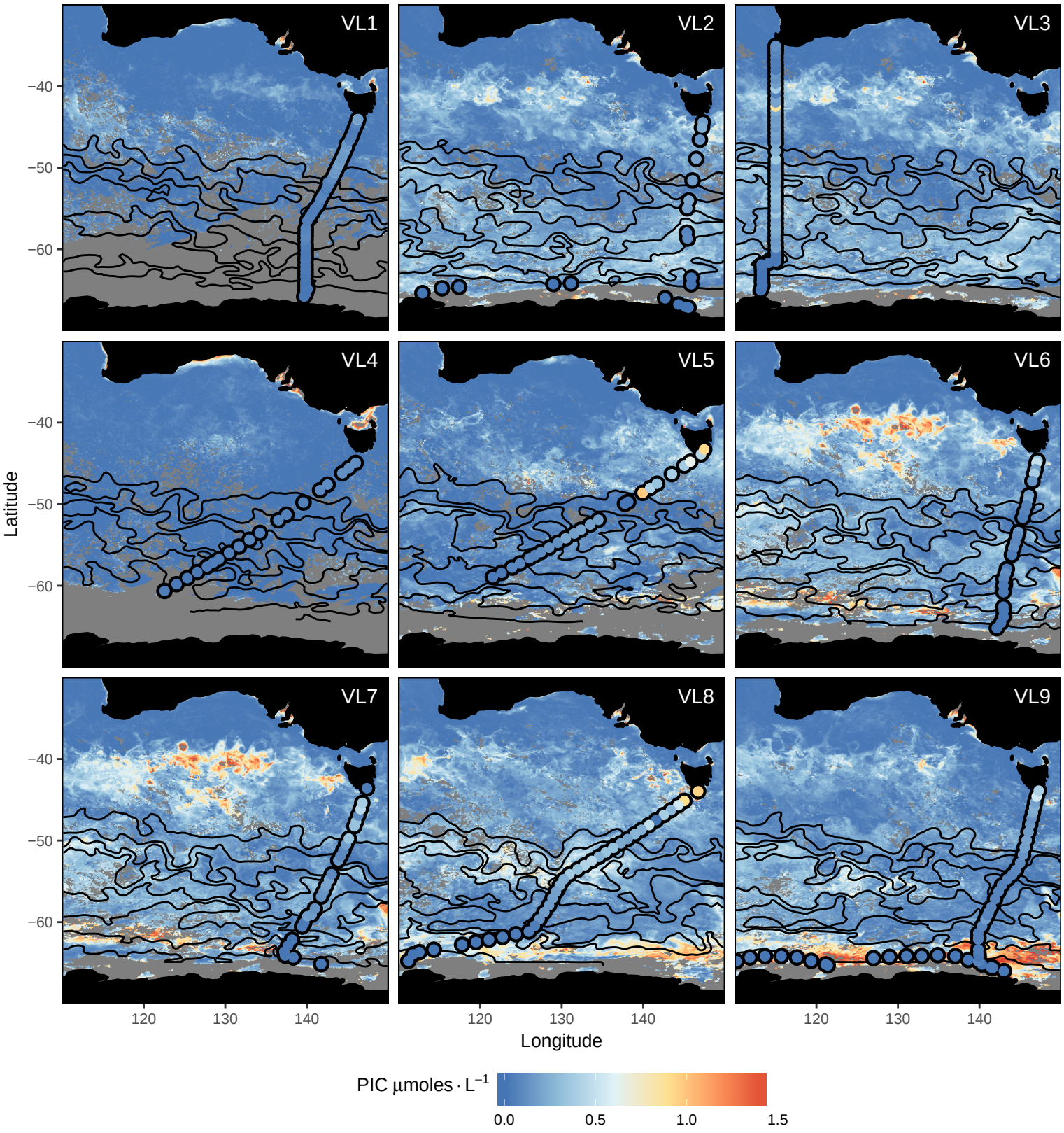
VL1
VL2
VL3
VL4
VL5
VL6
VL7
VL8
VL9
−40
−50
−60
Latitude
120
130
140
Longitude
PIC µmoles · L^{-1}
0.0
0.5
1.0
1.5

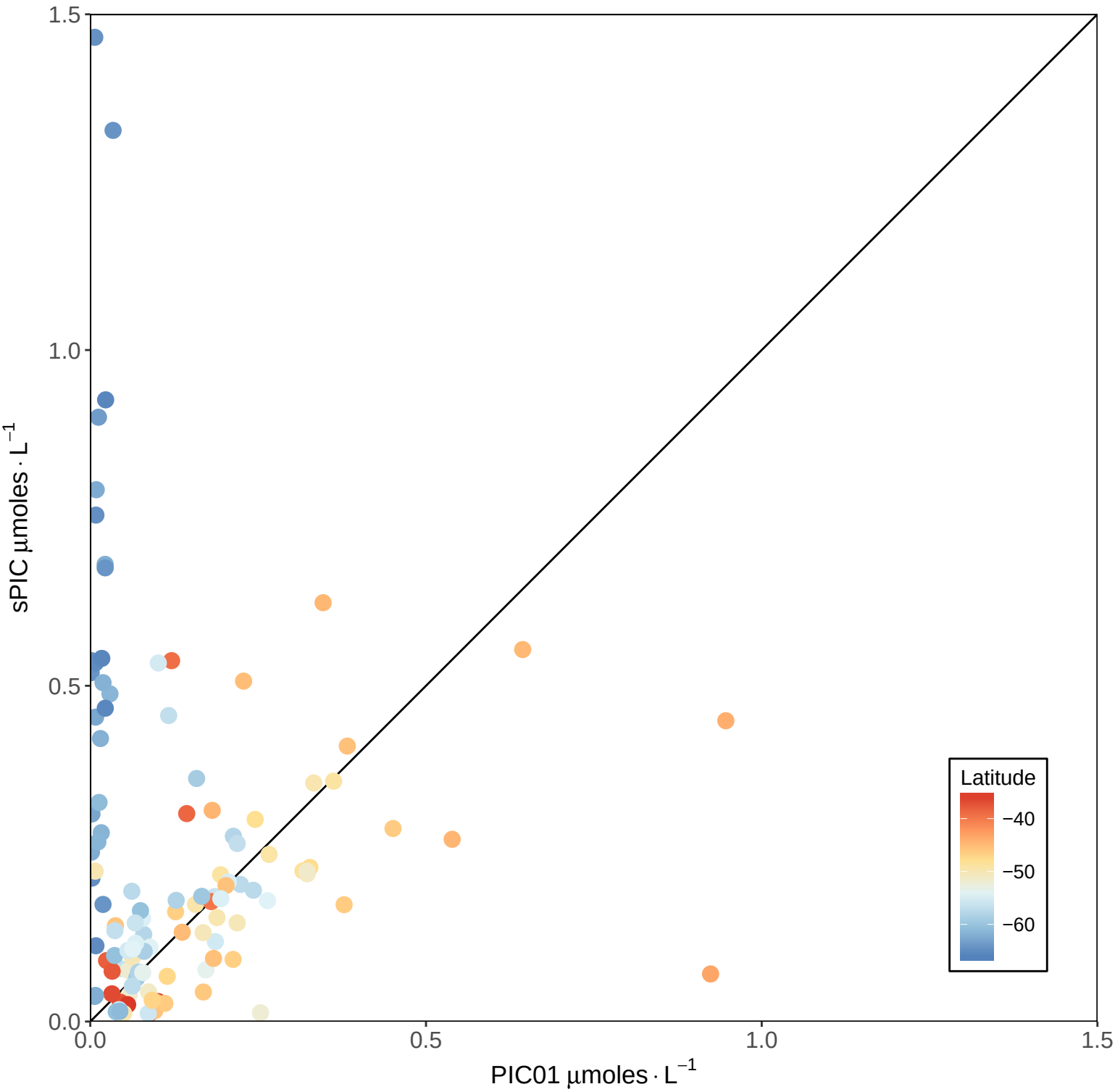
1.5
1.0
0.5
0.0
0.0
0.5
1.0
1.5
sPIC µmoles · L^{-1}
PIC01 µmoles · L^{-1}
Latitude
−40
−50
−60

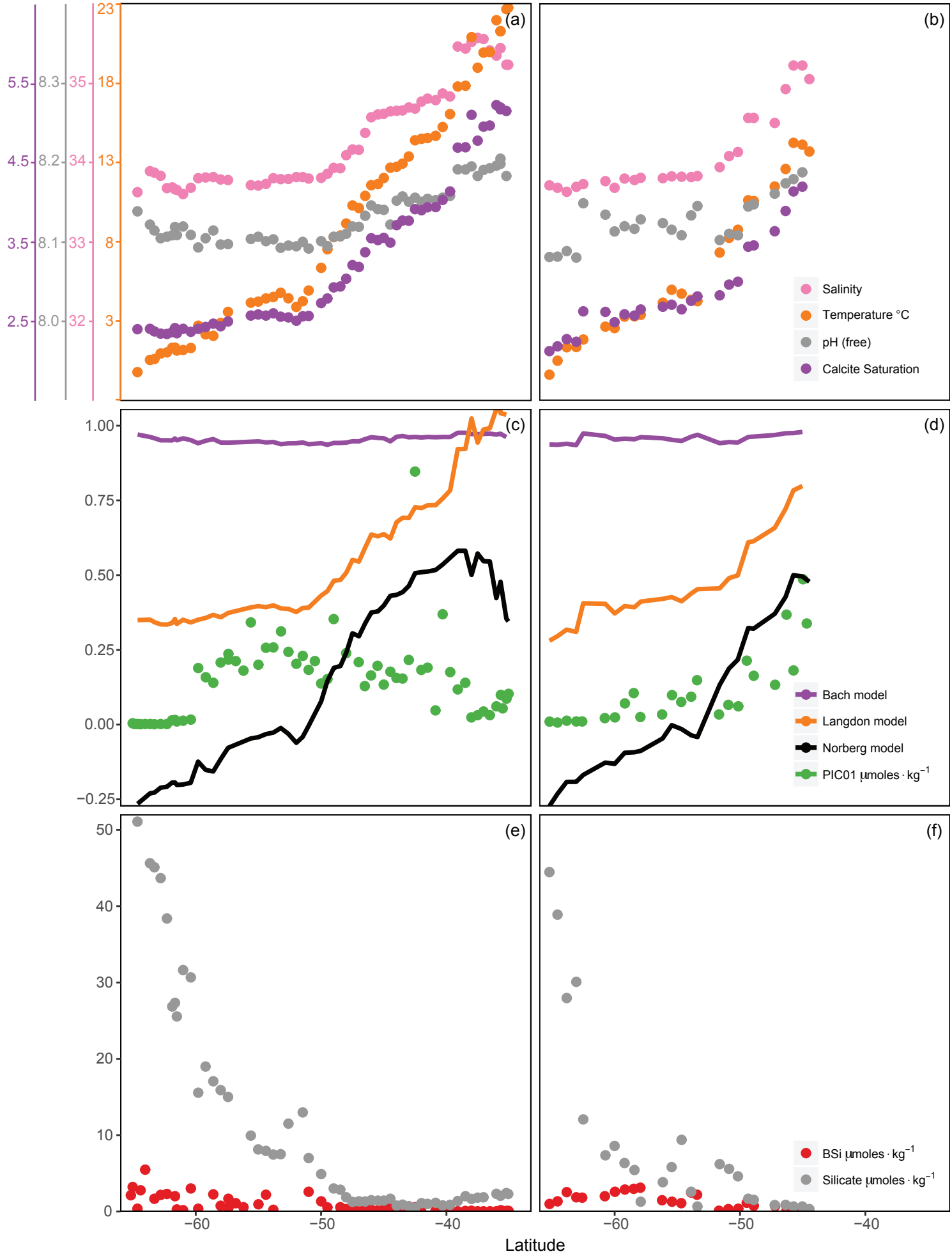
(a)
(b)
(c)
(d)
(e)
(f)
Salinity
Temperature °C
pH (free)
Calcite Saturation
Bach model
Langdon model
Norberg model
PIC01 µmoles · kg^{-1}
BSi µmoles · kg^{-1}
Silicate µmoles · kg^{-1}
Latitude

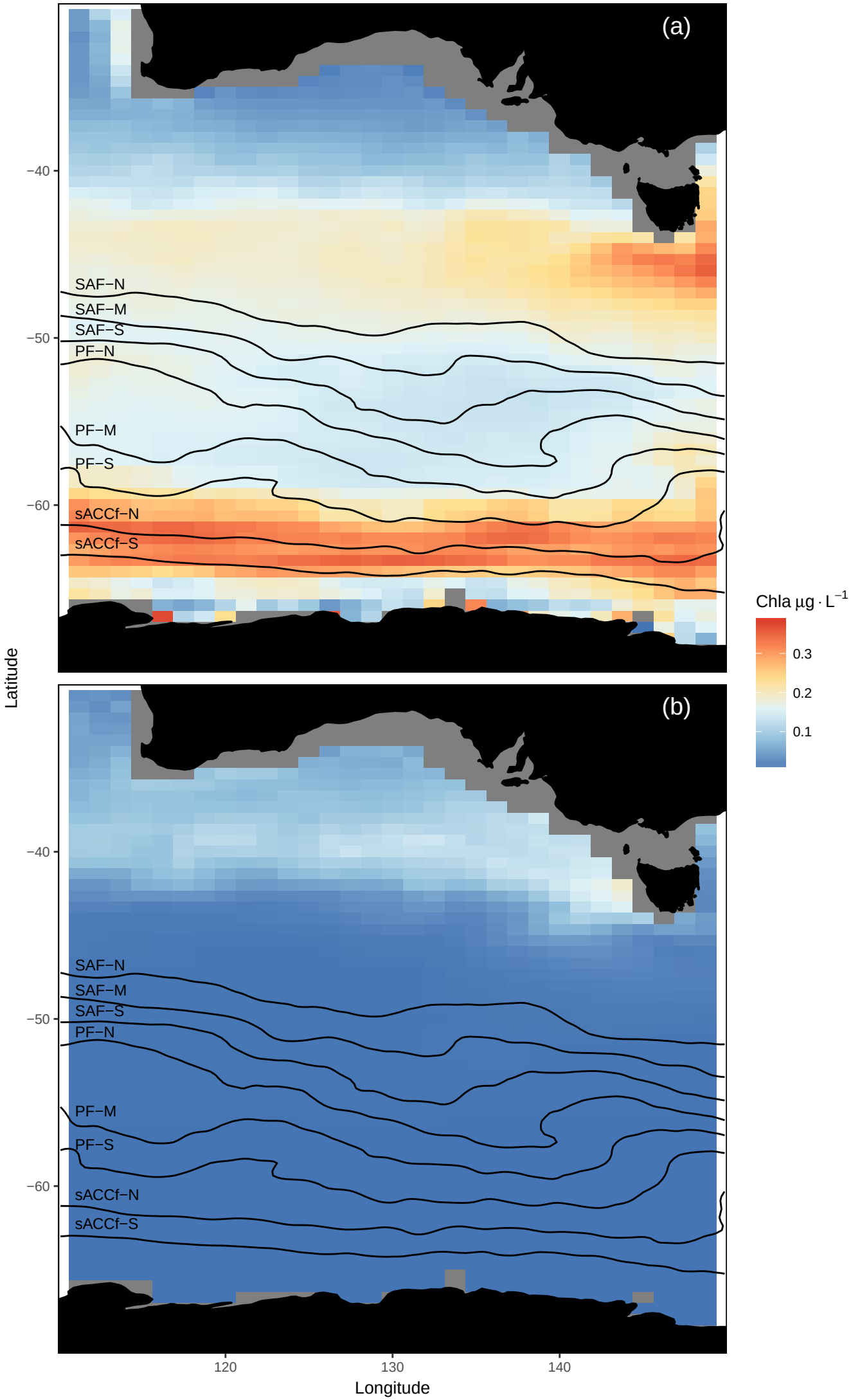
(a)
(b)
SAF−N
SAF−M
SAF−S
PF−N
PF−M
PF−S
sACCf−N
sACCf−S
−40
−50
−60
120
130
140
Latitude
Longitude
Chla µg · L−1
0.3
0.2
0.1